Developmental Biology

Extracellular adenosine deamination primes tip organizer development in *Dictyostelium*

Reviewed Preprint
v1 • March 11, 2025
Not revised

Pavani Hathi, Ramamurthy Baskar

Bhupat and Jyoti Mehta School of Biosciences, Department of Biotechnology, Indian Institute of Technology-Madras, Chennai, India

eLife Assessment

This **valuable** study identifies a protein called adenosine deaminase-related growth factor (ADGF) as a key regulator of tip formation in the slime mold Dictyostelium discoideum. The authors **convincingly** show that ADGF catalyses the formation of ammonia from adenosine, allowing ammonia to initiate tip formation, and then elucidate pathways upstream and downstream from ADGF. The authors discuss the intriguing possibility that mammalian ADGF may also similarly regulate development.

https://doi.org/10.7554/eLife.104855.1.sa3

Abstract

Ammonia is a morphogen in *Dictyostelium* and is known to arise from the catabolism of proteins and RNA. However, we show that extracellular adenosine deamination catalyzed by adenosine deaminase related growth factor (ADGF), is a major source of ammonia and demonstrate a direct role of ammonia in tip organizer development. The tip formed during early development in *Dictyostelium* is functionally similar to the embryonic organizer of higher vertebrates. *adgf* mutants fail to establish an organizer and this could be reversed by exposing the mutants to volatile ammonia. Interestingly, bacteria physically separated from the *adgf*$^-$ mounds in a partitioned dish also rescues the mound arrest phenotype suggesting a cross kingdom interaction driving development. Both the substrate, adenosine and the product, ammonia regulate *adgf* expression, and *adgf* acts downstream of the histidine kinase *dhkD* in regulating tip formation. Thus, the consecutive transformation of extracellular cAMP to adenosine, and adenosine to ammonia are integral steps during *Dictyostelium* development. Remarkably, in higher vertebrates, *adgf* expression is elevated during gastrulation and thus adenosine deamination may be an evolutionarily conserved process driving organizer development.

Introduction

During early embryonic development, organizers play an important role in patterning and directing the differentiation of surrounding cells into specific tissues and organs. The embryonic organizer establishes the developmental polarity in vertebrates and similarly, the mound/slug tip in *Dictyostelium* act as organizers (Rubin and Robertson, 1975) playing a pivotal role in guiding collective cell migration and patterning. Despite numerous investigations on *Dictyostelium* tip formation, the processes by which the tip establishes and maintains the primary developmental axis remains elusive. Gaining insights into the mechanisms regulating tip organizer function will offer a valuable understanding of the orchestrated cell movements and intricate processes underlying development.

Study of the social amoeba *Dictyostelium discoideum* has helped us to better understand many fundamental problems about development (Annesley and Fisher, 2009; Müller-Taubenberger et al., 2013; Dunn et al., 2018; Martín-González et al., 2021; Huber et al., 2022). *Dictyostelium* has demonstrated its value in a range of applications, including the investigation of human diseases (Eichinger et al., 2005; Müller-Taubenberger et al., 2013; Storey et al., 2022). *Dictyostelium* are free living, amoeboid, soil protists and alternate their life cycle between unicellular and multi- cellular stages. The amoebae prey on bacteria and upon starvation, the cells aggregate gradually forming a tipped multicellular mound. The mound further develops to form a slug which undergoes differentiation and morphogenesis to form a fruiting body consisting of a dead stalk supporting a ball of spores (Raper, 1940; Kessin, 2001).

Diffusible molecules such as cAMP, adenosine, ammonia, and a chlorinated hexaphenone 'differentiation-inducing factor' (DIF) regulate multicellular development in *Dictyostelium* (Bloom and Kay, 1988; Williams, 1988; Gross, 1994; Mahadeo and Parent, 2006; Shu et al., 2006). The gradient of these morphogens along the slug axis determines the cell fate, either as prestalk (pst) or as prespore (psp) cells. cAMP regulates PKA activity, adenosine signaling, and morphogenetic cell movements to control tip development in *Dictyostelium* (Mann and Firtel, 1993; Siegert and Weijer, 1995). Adenosine, a by-product of cAMP hydrolysis, acts as an inhibitory morphogen suppressing additional tip formation (Schaap and Wang, 1986), however the mechanism involved in tip formation is not completely understood.

Adenosine deaminase (ADA) or its isoforms regulate adenosine homeostasis by catalysing the breakdown of adenosine to generate inosine and ammonia, and are conserved among bacteria, invertebrates, vertebrates including mammals (Cristalli et al., 2001). Two isoforms of ADA are known in humans including ADA1 and ADA2 and ADGF shares a structural similarity to ADA2. ADA2 is associated with the activation of lymphocytes that play a role in the immune response to infections (Marone et al., 1980). Absence of ADA2 activity results in the build-up of deoxyadenosine and its phosphorylated metabolite, dATP that is toxic to lymphoid precursors (Notarangelo, 2016). Consequently, complete ADA2 deficiency is characterized by lymphopenia and severe combined immuno-deficiency disorder (SCID) (Gaspar, 2010). The loss-of-function mutations in *adgf/ada2* in humans also manifest in a variety of vascular and inflammatory symptoms, including early-onset of stroke and systemic vasculopathy (Zhou et al., 2014).

ada2 disruption in mice leads to liver dysfunction and perinatal mortality (Wakamiya et al., 1995) and transgenic overexpression of ADA2 in mice results in aberrant heart and kidney development (Riazi et al., 2005). Absence of *adgf/ada2* in frogs manifests in reduced body size with altered polarity (Iijima et al., 2008). In *Drosophila*, six ADGFs have been identified and are reported to promote cell proliferation by depleting extracellular adenosine (Zurovec et al., 2002). Loss of function of *adgfA* in *Drosophila* promotes melanotic tumour formation and larval death (Dolezal et al., 2005). In *Arabidopsis thaliana*, tRNA adenosine deaminase 3 (*tad3*) is

necessary for telomere length homeostasis (Bose et al., 2020). Adenosine deaminases are known to interact with dipeptidyl peptidase IV (DPP), CD26 (cluster of differentiation 26) expressed on T-cells and the adenosine receptor, A2AR (expressed on dendritic cells) to facilitate cell-cell signaling (Moreno et al., 2018). Thus, *adgf* plays a pivotal role in the regulation of cell proliferation and development in several organisms.

Four isoforms of ADA are annotated in the *Dictyostelium discoideum* genome (Eichinger et al., 2005) including adenosine deaminase (*ada*; DDB_G0287371), adenosine deaminase acting on tRNA-1 (DDB_G0278943), adenosine deaminase tRNA-specific (DDB_G0288099) and adenosine deaminase-related growth factor (*adgf*; DDB_G0275179), and their role in growth and development is not known. In this study, we examined the role of *adgf* during multicellular development in *D. discoideum* and demonstrate that ammonia derived from adenosine deamination is directly involved in tip organizer development.

Results

Differential regulation of *adgf* expression during growth and development

To verify the blasticidin *(bsr)* insertion in *adgf*$^{-}$, a diagnostic PCR was carried out and the integration was validated (**Figures 1A** and **1B**), and qRT-PCR analysis confirmed the absence of *adgf* expression (**Figure 1C**). In vertebrates, adenosine deaminases are expressed in a tissue specific manner to control growth and development. To know if *adgf* expression is differentially regulated during development in *Dictyostelium*, qRT-PCR was performed using RNA obtained from different stages of development. The time point of analysis includes 0 h, 8 h, 12 h, 16 h, 20 h and 24 h. *adgf* expression peaks at 16 h (**Figure 1D**) implying an important role for *adgf* later in development. At this time point, the expression of the other three isoforms of ADA were not significantly different from WT, suggesting that they do not compensate for the loss of *adgf* (**Figure 1E**).

Dictyostelium ADGF shares a strong structural similarity with human ADA2

The *D. discoideum adgf* gene is predicted to encode a protein of 543 long amino acids and belongs to the metallo-transferase superfamily (**Figure 2A**), containing a ADA domain and an N-terminal domain similar to human ADA2 (**Figure 2B**). Using the ADGF sequence from the protein family database (*https://www.ebi.ac.uk/interpro/*), an analysis was carried out using the online tools, SMART (Simple Modular Architecture Research Tool: *http://smart.embl-heidelberg.de*), to know the presence of structurally similar domains. This study suggests that the protein domains of *Dictyostelium* ADGF are conserved and show high degree of similarity with human *ada2*.

D. discoideum ADGF (DdADGF) shares 37.47% identity with human ADA2. ADGF is present in other social amoeba, sharing a sequence similarity of 59.5% with *Dictyostelium fasciculatum*, 61.2% with *Dictyostelium pupureum*, 53.6% with *Dictyostelium lacteum* and 62.1% with *Polysphondylium pallidum* (*www.uniprot.org*). Multiple sequence alignment reveals the presence of an N-terminal signal sequence characteristic of extracellular proteins (**Figure 2C**) and conserved histidine and glutamine residues in the active site of both *D. discoideum* ADGF and human ADA2 (**Figure 2D**).

The phylogenetic relation of ADGF to the classic ADA subfamily has been reported previously (Maier et al., 2005). To determine the evolutionary relationship of *D. discoideum* ADGF with that of other organisms, a phylogenetic analysis was carried out and the alignment was created using

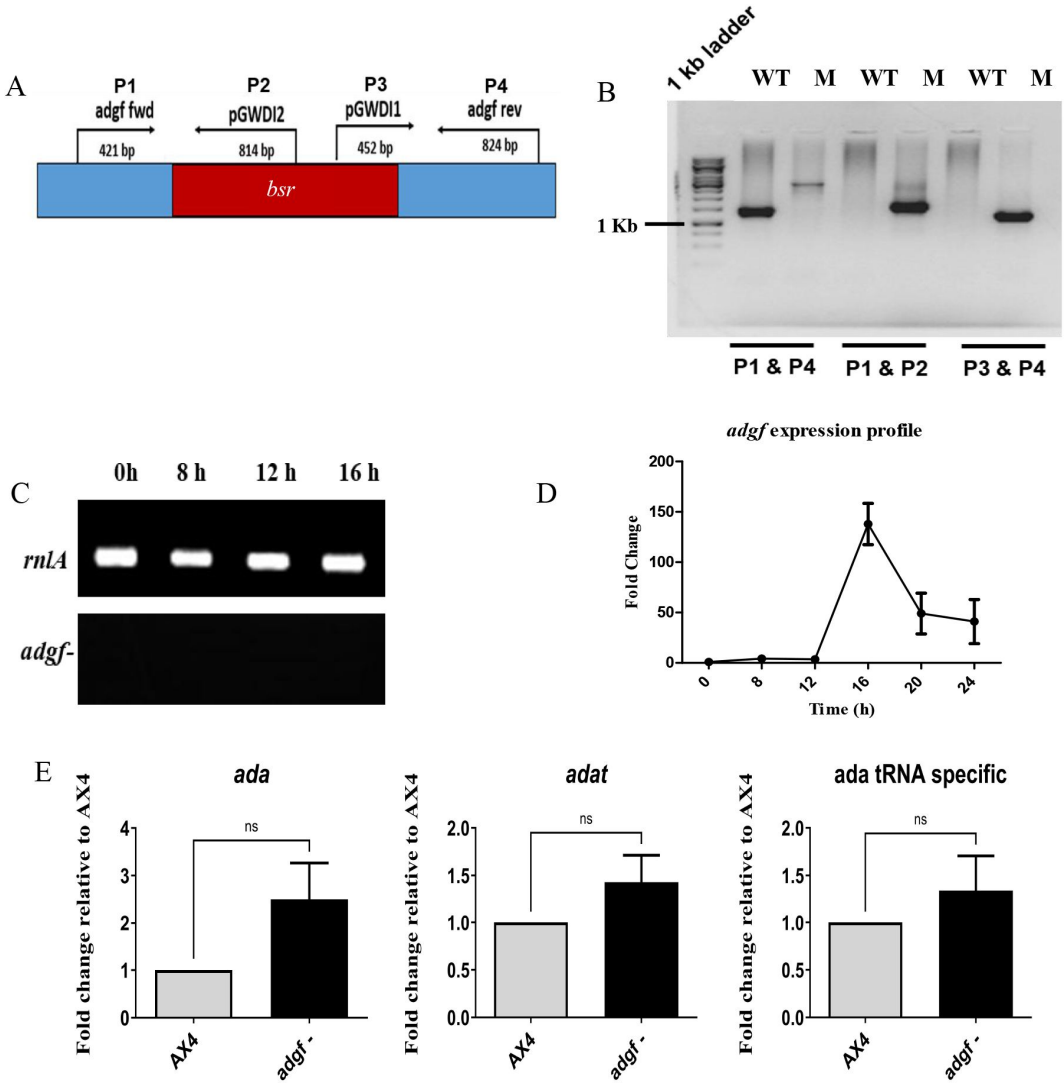

Figure 1.

Mutant validation.

A) Blasticidin resistance cassette (*bsr*) insertion in the *adgf* gene. **B)** PCR analyses using P1 and P4 primers. 1.4 kb shift in the *adgf* mutant. PCR using P1 and P2 primers showed an amplicon from the mutant (M) and not from the wild type (WT). PCR using P3 and P4 primers showed an amplicon with adgf mutant while WT did not show any amplicon. **C)** Semi- quantitative RT-PCR of internal control, *rnlA* and *adgf* $^{-}$. *adgf* expression during development in *Dictyostelium*. **D)** Total RNA was isolated from *Dictyostelium* during vegetative growth and development using TRIzol method. To quantify *adgf* expression, qRT-PCR was carried out with *rnlA* as a control and the fold change was calculated accordingly. Time points are shown in hours (bottom). Error bars represent the mean and SEM (n = 3). **E)** RT-PCR analysis was performed to check the expression of the isoforms of ADA during 16 h in the mutant.

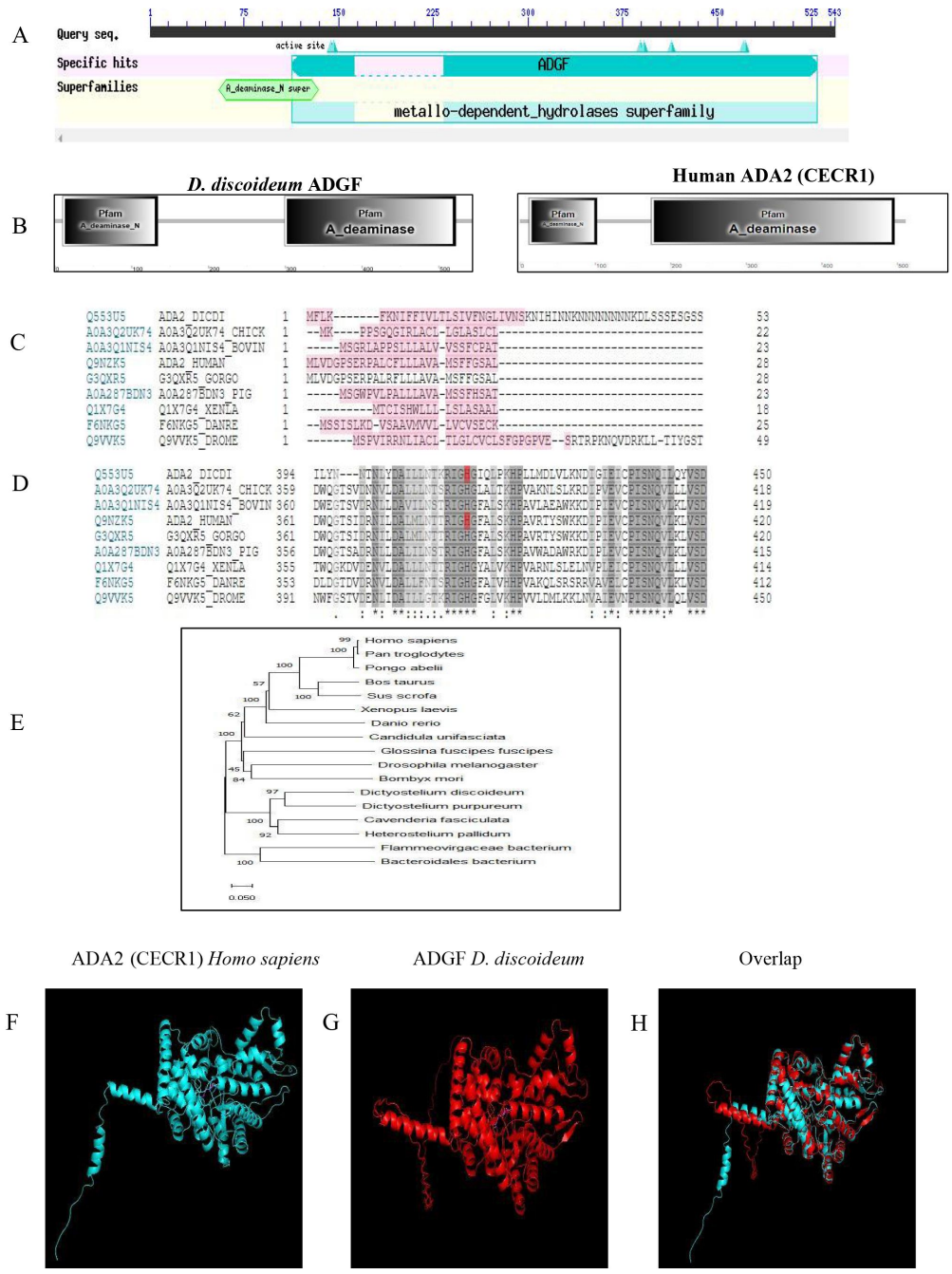

Figure 2.

Bioinformatic analyses of ADGF.

A) BLAST analysis of ADGF. ADGF belongs to the metallo dependent hydrolases superfamily.
B) SMART analysis of different ADA domains within ADGF. ADGF protein has an adenosine deaminase-ADA domain and a N-terminal deaminase domain which is similar to the human ADA2. **Multiple sequence alignment of *Dictyostelium* ADGF with ADGF from other organisms. C)** The shaded region depicts the N-terminal signal sequence characteristic of extracellular proteins. **D)** The active site residue is highlighted in red. Active site residue is conserved between *D.discoideum* and human *ada2*. **E)** Phylogenetic analysis of ADGF across different organisms. Maximum likelihood method was used for constructing the tree using MEGAX (Molecular Evolutionary Genetic Analysis X). **Structural Comparison of human ADA2 and *Dictyostelium* ADGF.** Identical tertiary structures of human ADA2 and *Dictyostelium* ADGF. **F)** ADA2 (CECR1) *Homo sapiens* and **G)** ADGF *Dictyostelium discoideum* have many structural similarities. **H)** Alignment of *Dictyostelium* ADGF with Human ADA2 (CECR1).

MEGAX software (Kumar et al., 2018). The evolutionary history of ADGF was inferred using a Maximum Likelihood approach with Bootstrap analysis (100 iterations) as described by Felsenstein (1985). The resulting phylogenetic tree indicated that DdADGF is closely related to the ADGF proteins of other Dictyostelid members, including D. purpureum, Heterostelium pallidum, and Cavenderia fasciculata. *D. discoideum* ADGF forms a distinct clade, likely representing a distant relative of its vertebrate homolog (**Figure 2E**). Additionally, the structure of *D. discoideum* ADGF was predicted by homology modeling with AlphaFold (*https://alphafold.ebi.ac.uk/*), using the crystal structure of human ADA2, CECR1 (Cat eye syndrome critical region protein 1) as a template (PDB-3LGD) (**Figures 2F-H**). Alignment of *Dictyostelium* ADGF with human ADA2 yielded an RMSD value of 1.003 Å, indicating strong structural similarity (Eidhammer et al., 2000; Koehl, 2001).

adgf controls aggregate size in *Dictyostelium*

To understand the role of *adgf* during *D. discoideum* development, mutant lines with lesions in the gene *adgf* were plated at a density of $5x10^5$ cells/cm^2 on non-nutrient phosphate buffered agar plates (pH 6.4) and monitored thereafter. In comparison to WT (37.6 ± 2.7 mm^2), the aggregates of *adgf*$^-$ were larger in size (62.6 ± 5.4 mm^2; p value = 0.0003), and thus the number of aggregates formed by the mutants were fewer (39.67 ± 3.703) than the WT (67.00 ± 2.543) (**Figure 3A**). To determine the pathways that are affected impairing the tissue size in the mutant, RNA expression of countin (*ctn*) and small aggregates (*smlA*) were examined and their levels were found to be reduced significantly compared to controls (**Figure 3B**). Countin factor (CF) regulates group size by reducing the expression of cell-cell adhesion proteins cadherin (*cadA*) and contact site A (*csaA*) (Siu et al., 1985). The expression of *cadA*, *csaA* and cell-cell adhesion were also quantified and the mutants displayed enhanced *cadA* and *csaA* expression and higher cell-to-cell contacts than the WT (**Figures 3C** and **3D**) suggesting that *adgf* regulates the overall size of the aggregates.

cAMP chemotaxis significantly influences cell-cell adhesion (Konijn et al., 1967) and to know if chemotaxis is impaired in the mutant, an under-agarose chemotaxis assay was carried out. The chemotactic activity was not significantly different between the two cell types (**Figure 3E**), implying that the increased mound size in the mutant may not be due to altered chemotactic activity.

adgf mutants form large, tipless mounds

Subsequent to plating on KK2 agar plates, WT cells formed mounds by 8-9 h, and culminate to form fruiting bodies by the end of 24 h. In contrast, the *adgf*$^-$ lines were blocked as rotating mounds with no tips till 30 h (**Figure 3F**; Supplementary videos S1 and S2). The mound arrest phenotype could be mimicked by adding the ADA specific inhibitor deoxycoformycin (DCF) to WT cells (**Figure 3G**). After 36 h, a fraction of *adgf*$^-$ mounds (34.77 ± 4%) formed fruiting bodies with bulkier spore sac and a stalk (**Figures 3H** and **3I**). This late recovery from the mound arrest may be due to the expression of other ADA isoforms after 36 h.

Reduced ADA activity leads to high adenosine levels in the *adgf* mutant

If the function of *adgf* is compromised, ADA enzyme activity is expected to be low. To verify this, total ADA activity in WT and *adgf*$^-$ mounds was measured using a commercial kit. This technique relies on the conversion of inosine (by ADA) to uric acid and was measured at A293 nm. Although ADA activity was reduced significantly in the mutant (**Figure 4A**), it was not completely abolished and possibly, other isoforms of ADA may have a basal activity at 16 h.

ADGF quenches extracellular adenosine and if this process is impaired as expected in *adgf*$^-$, the mutants will have increased extracellular adenosine. Using a commercial kit, total adenosine levels were measured and the adenosine levels were elevated both at 12 h and 16 h in the mutant,

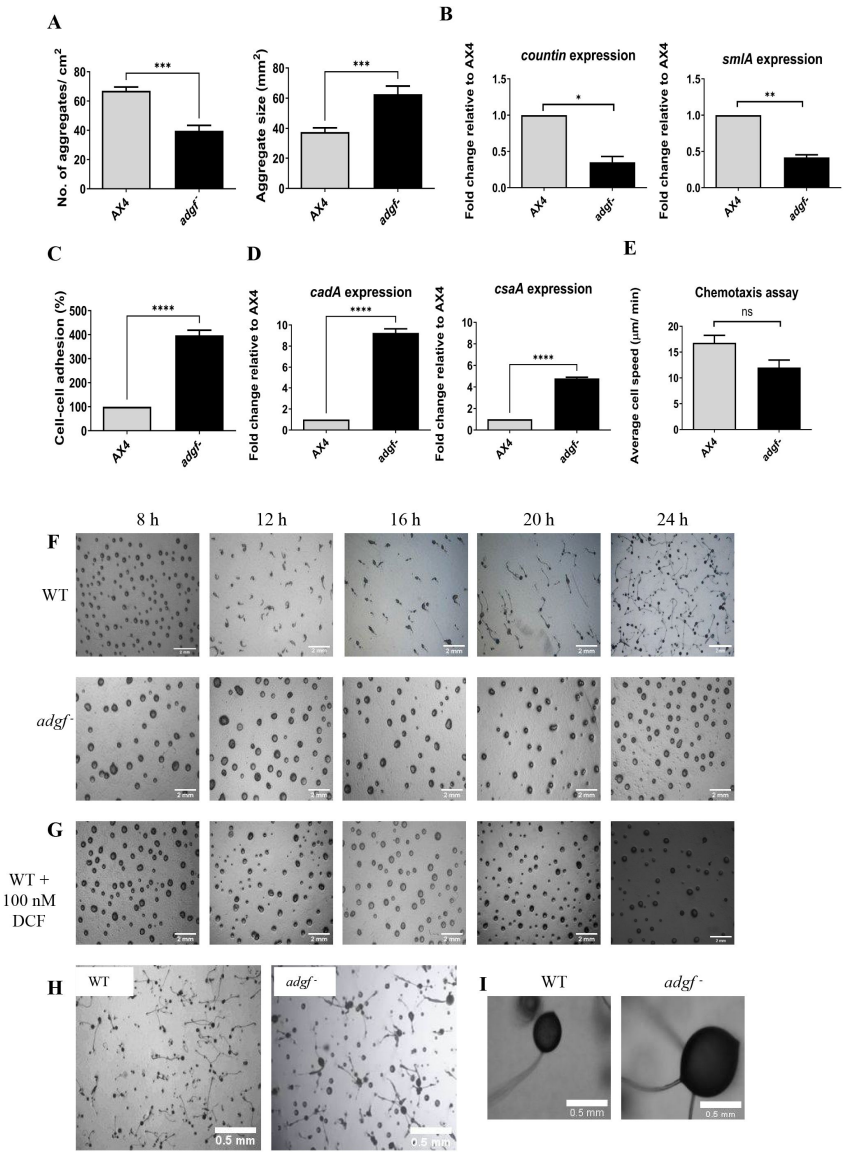

Figure 3.

Aggregates formed by *adgf*¯ mutants are larger in size.

A) The graph shows the number of aggregates formed by WT and *adgf* ¯ and their respective mound size. The values represent mean ± S.E; n=3. Significance level is indicated as *p< 0.05, **p< 0.01, ***p< 0.001, ****p< 0.0001. (Student's t-test). **B)** Expression levels of genes countin (*ctn*) and small aggregates (*smlA*) during aggregation in *adgf* ¯ compared to WT. *rnlA* was used as the internal control in the realtime PCR. **C)** WT and *adgf* ¯ cells were developed on KK2 agar, and after 16 h, the multicellular mounds/slugs were dissociated by vigorous vortexing in KK2 buffer. Individual cells were counted using a hemocytometer and resuspended in a phosphate buffer. Non-adherent single cells were counted 45 min after incubation. The percent cell-cell adhesion was plotted by normalizing the values to the non-adherent WT count to 100%. Error bars represent the mean ± SEM (n=3). Cell-cell adhesion, but not cAMP chemotaxis, is significantly impaired in *adgf* ¯. **D)** qRT-PCR analysis of cadherin (*cadA*) and contact site (*csA*) during aggregation. The fold-change in RNA transcript levels is relative to WT at the indicated time points. *rnlA* was used as the internal control (n=3). ns = not significant. **E)** Under agarose chemotaxis assay: The average cell speed in response to 10 µM cAMP was recorded. The graph represents the mean ± SEM (n=3). **Developmental phenotype of *adgf* ¯. F)** WT and *adgf* ¯ cells were washed, plated on 1% KK2 agar plates at a density of $5x10^5$ cells/cm^2, incubated in a dark, moist chamber and images were taken at different time intervals. **G)** WT cells treated with 100 nM of DCF mimicked the mound arrest phenotype of the mutant. The time points are indicated in hours at the top of the figure. Scale bar: 2 mm; (n=3). **H)** WT and *adgf* ¯ cells after 36 h of development. Scale bar: 0.5 mm; (n=3). **I)** Fruiting bodies of WT and *adgf* ¯. Scale bar: 0.5 mm; (n=3).

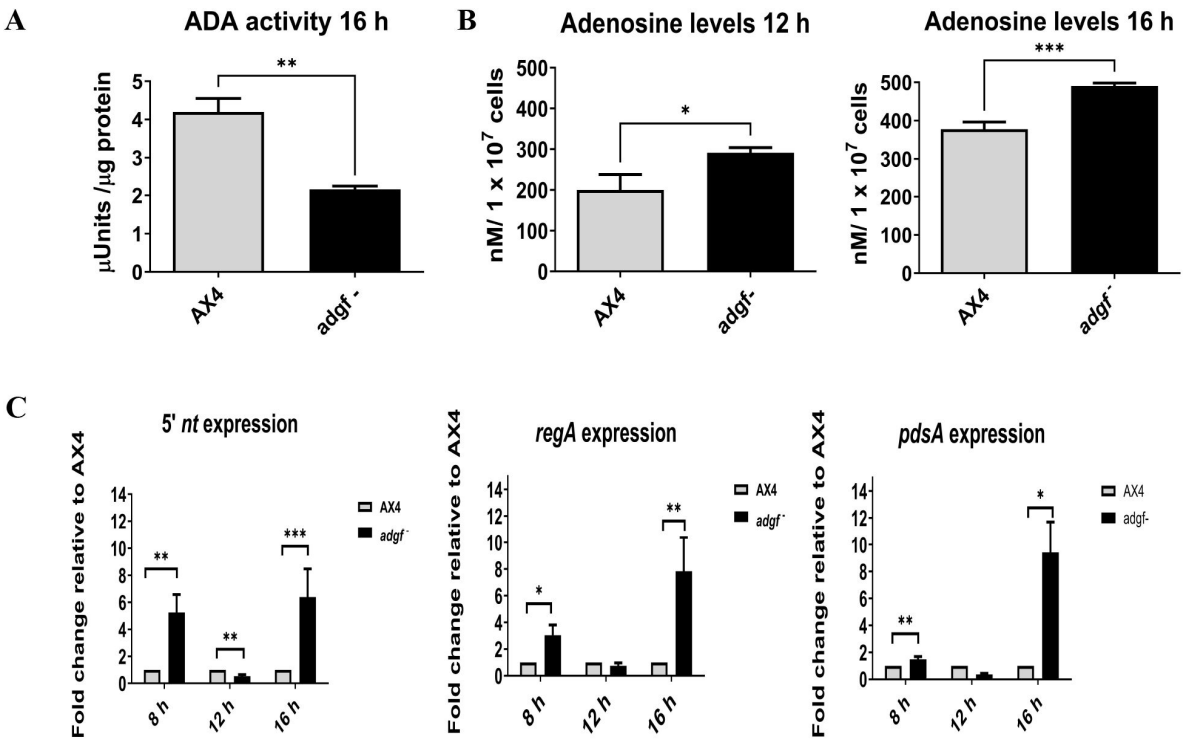

Figure 4.

Reduced ADA activity and high adenosine levels in *adgf*$^{-}$.

A) ADA activity in *Dictyostelium* cell extracts harvested at 16 h. The enzymatic assay for ADA was performed in *adgf*$^{-}$ with the corresponding WT control. Error bars represent the mean and SEM (n=3). Significance level is indicated as *p< 0.05, **p< 0.01. Adenosine quantification and expression profile of genes involved in adenosine formation. **B)** Quantification of adenosine levels. Level of significance is indicated as *p< 0.05, **p< 0.01, ***p< 0.001; (n=3). **C)** Expression profile of the genes, 5' nucleotidase (5'*nt*) and phosphodiesterases (*regA*, *pdsA*) involved in cAMP-to- adenosine conversion. The fold-change in RNA transcript levels is relative to WT at the indicated time points. *rnlA* was used as an internal control. Error bars represent the mean and SEM (n=3).

(**Figure 4B**) and this difference was highly significant at 16 h (377.6 ± 18.86 nM in the WT; 490.8 ± 7.241 nM in the mutant, p = 0.0002). *adgf* expression, at this time point was also high in WT cells. The elevated adenosine levels at 16 h may be due to reduced ADA activity and enhanced expression of genes such as 5' nucleotidase (*5'nt),* phosphodiesterases *(pdsA* and *regA)* that are involved in adenosine formation. Hence, their expression levels were examined. Although the expression of both *5'nt* and *regA* were enhanced at 8 h, *pdsA* levels remain unaltered. Interestingly, the expression of all three genes trended lower at 12 h but were significantly upregulated at 16 h (**Figure 4C**) suggesting an important role of these genes at a specific time in development.

Addition of ADA or overexpression of *adgf* cDNA restored tip development in *adgf*¯

adgf mutants carry significantly high levels of adenosine. By administering ADA enzyme on top of the *adgf*¯ mounds (**Figure 5A**), excess adenosine can be quenched resulting in ammonia formation, possibly rescuing the phenotype. Indeed, addition of 10 U ADA onto mutant mounds restored tip development. Besides, overexpression of WT *adgf* cDNA (driven by actin15 promoter) rescues the developmental defects of the *adgf* mutants (**Figures 5B** and **5C**), confirming that the developmental block is the result of *adgf* gene disruption alone. However, *adgf* cDNA overexpression in WT cells does not result in any observable defects (**Figure 5D**). Taken together, these findings support an important function of *adgf* in tip development.

WT or its conditioned media (CM) restored tip formation in *adgf*¯ mounds

In order to determine whether *adgf* is necessary for tip formation in a cell-autonomous manner, WT and the mutant cells were reconstituted in different proportions and plated. In a mix of 50% WT: 50% mutant, WT cells were able to rescue the defects of *adgf*¯ cells but with 20% WT and 80% *adgf*¯, the rescue was partial (31 ± 4 %) (**Figure 5E**) suggesting that the mound arrest phenotype of the mutant is due to the absence of some secreted factor(s).

Further, when developed in the presence of WT CM, *adgf*¯ cells formed tipped mounds and eventually fruiting bodies (**Figure 5F**). Conversely, in the presence of CM from *adgf*¯ cells, WT developed as large mounds with no tips (**Figure 5G**) and the size was comparable to the mounds formed by *adgf*¯. These findings imply that the developmental phenotype of *adgf*¯ is not due to a cell autonomous defect but due to faulty secreted factor signaling.

Volatile ammonia rescued the mound arrest phenotype of *adgf*¯

If ADGF function is compromised, ammonia levels are expected to be low. Hence, the concentration of ammonia from WT and *adgf*¯ mounds were measured using a commercial kit. At the mound stage, total ammonia levels were significantly reduced in *adgf*¯ lines (**Figure 6A**). By mixing sodium hydroxide and ammonium chloride (Thadani et al., 1977), ammonia could be generated, and in such conditions, tip formation was restored in *adgf*¯ mounds (**Figure 6B**).

Physically separated WT restored tip development in the mutant

WT mounds are expected to release lot of volatiles including ammonia, possibly rescuing the mound arrest phenotype of the mutants nearby. To verify if this is correct, *adgf*¯ cells were developed in one half of a compartmentalized Petri dish and WT cells on the other side. Interestingly, the mound arrest of *adgf*¯ was completely rescued by 3.5 hours (**Figure 6C**) in the

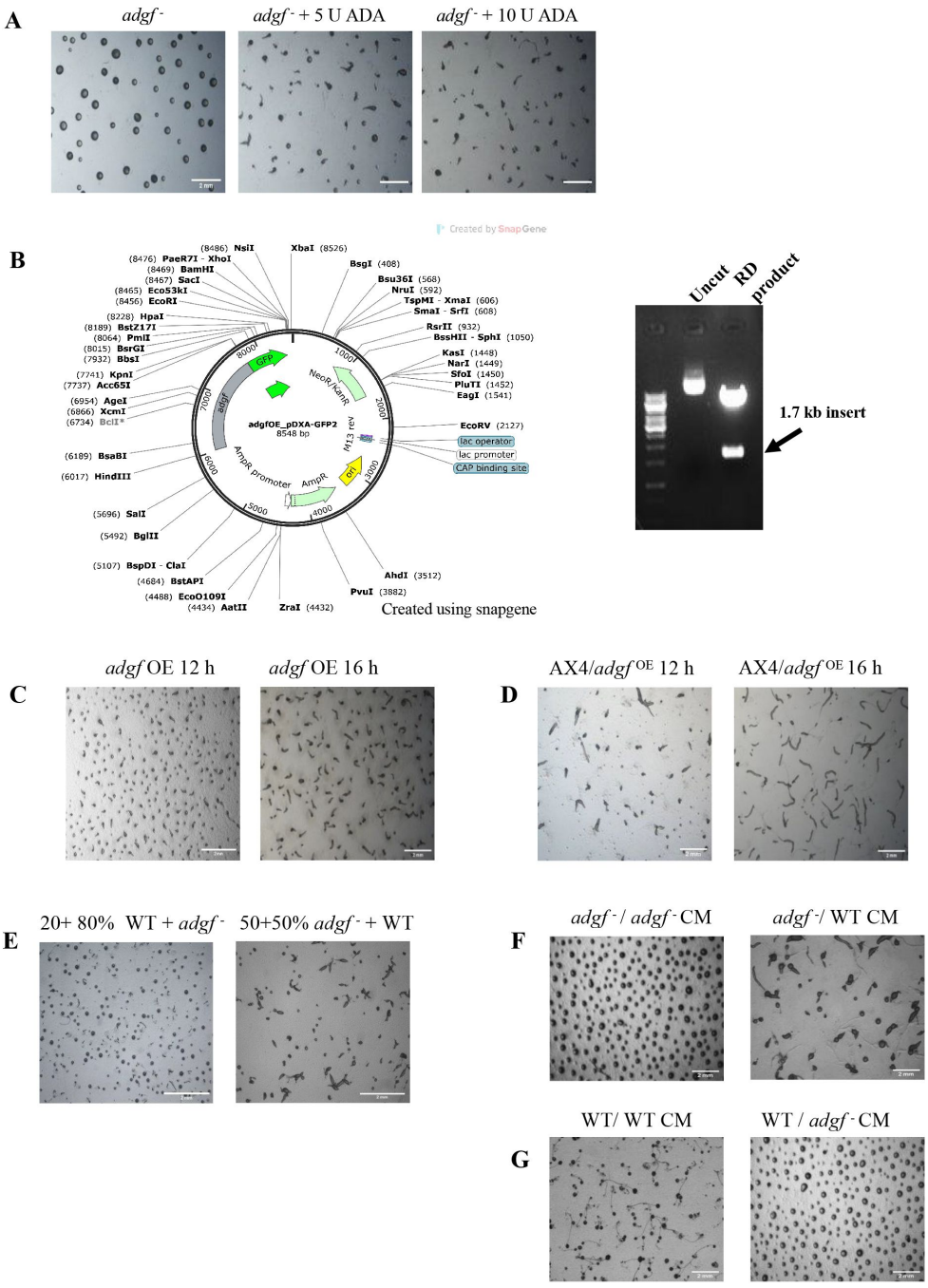

Figure 5.

Overexpression of *adgf* rescued the mound arrest phenotype.

A) *adgf*⁻ mounds were treated with 5 U and 10 U ADA enzyme, plated for development and imaged at 16 h. Scale bar: 2 mm; (n=3). **B)** The full-length *adgf* gene was cloned in the vector pDXA-GFP2. The overexpression construct was verified by restriction digestion with HindIII and Kpn1 enzymes.**C)** Overexpression of *adgf* in the mutant rescued the mound arrest. **D)** Overexpression of *adgf* in the WT background. Scale bar: 2 mm; (n=3). The time points in hours are shown at the top. **WT cells reconstituted with *adgf*⁻ rescued the *adgf* mutant phenotype. E)** Reconstitution of WT with *adgf*⁻ in a 1:4 ratio showing a partial rescue and a full rescue of the *adgf*⁻ mound arrest phenotype in a 1:1 ratio with WT. **F)** Development of *adgf* mutants in the presence of *adgf*⁻ CM and WT CM on KK2 agar plates. WT CM rescued the mound arrest. **G)** Development of WT in the presence of WT CM and *adgf*⁻ CM on KK2 agar plates. *adgf*⁻ CM induced mound arrest in WT cells. Scale bar: 2 mm; (n=3).

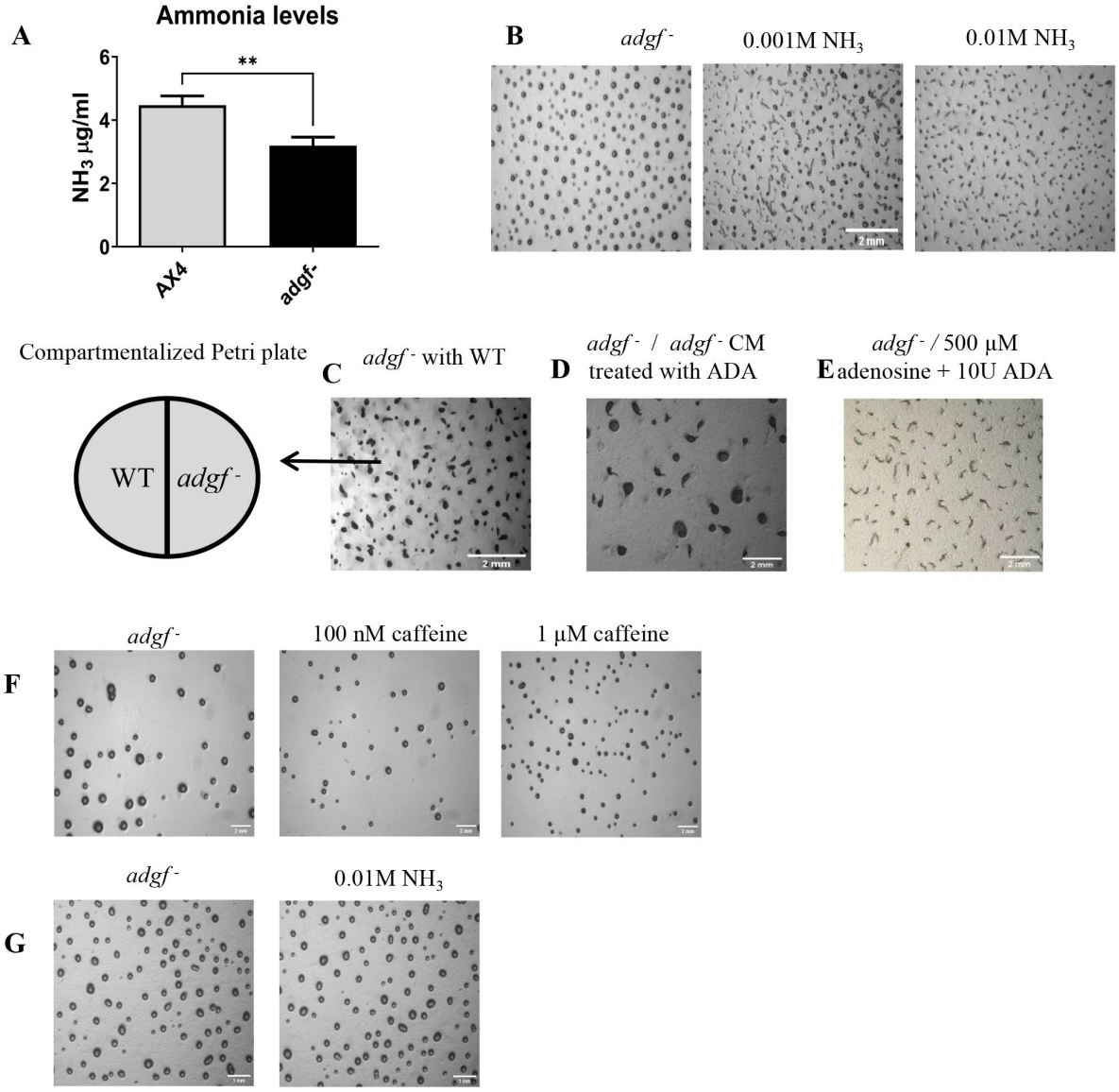

Figure 6.

Adenosine deamination reaction rescues the mound arrest of *adgf*¯.

A) Quantification of ammonia using the ammonia assay kit. WT and *adgf* ¯ mounds were harvested and lysed using a cell lysis buffer. Cell debris were removed by centrifugation, and the supernatant was used to quantify ammonia.
B) Exposing *adgf* ¯ mounds to ammonia. Ammonia was generated by mixing 2 ml of NH_4Cl and 2 ml of 1N NaOH. The mixture was poured on top of the lid and the KK2 plates with the mounds were inverted and sealed thereafter. Images were taken 3.5 h post treatment. Dose dependent effect of ammonia on the rescue. Scale bar: 2 mm; (n=3). **C)** WT and *adgf*¯ cells on either side of a compartmentalized Petri dish. **D)** *adgf*¯ cells on one side of the plate in the presence of *adgf*¯ CM treated with ADA enzyme in the other half of the dish. **E)** *adgf*¯ cells on one side and KK2 buffer containing adenosine and ADA on the other half of the compartmentalized dish, rescued the mound defect. **Caffeine rescues the large mound size of *adgf* mutant**. **F)** *adgf* ¯ cells were treated with different concentrations of caffeine (100 nM, 1 µM) while plating and images were taken 3.5 h post chemical treatment. Scale bar: 2 mm; n=3. **G)** Exposure to ammonia does not rescue the aggregate size of *adgf* mutant. *adgf* - mounds were exposed to 0.01 M ammonia and images were taken 3.5 h post chemical treatment. Scale bar: 2 mm; (n=3).

presence of WT although they were physically separated from each other. This suggests that volatiles, likely to be ammonia released from WT is sufficient enough to rescue the mutant phenotype.

The CM from *adgf*¯ is expected to have high adenosine, possibly generating low or no ammonia. Addition of ADA to the CM of the mutant in one compartment of the partitioned dish led to a partial rescue (57 % ± 2) of *adgf*¯ kept on the other side of the dish after 3.5 h (**Figure 6D**) implying that the ammonia generated in such conditions may not be enough for a full rescue.

Adenosine deamination alone drives the rescue of *adgf*¯

To know if adenosine deamination is exclusively responsible for the rescue of the mutant, 10 ml cold KK2 buffer mixed with different concentrations of adenosine (10 μM, 0.1 mM, 1 mM) was added on one side of the compartmentalized dish and the other side of the dish had the mutant on phosphate buffered agar arrested at the mound stage. After 3.5 h of the addition of ADA enzyme (10 U) to the buffered solution containing adenosine, a full rescue was observed (**Figure 6E**), strongly indicating that volatile ammonia generated from adenosine deamination alone is rescuing the defect. Ammonia is known to be produced during protein/RNA catabolism in *Dictyostelium* (White and Sussman, 1961; Hames and Ashworth, 1974; Schindler and Sussman, 1977; Walsh and Wright, 1978) but the total protein and RNA levels were not significantly different between WT and *adgf* mutants (Figure S1 A-B) suggesting that ammonia released from adenosine deamination plays a crucial role in tip formation.

Caffeine, not ammonia rescued the mound size of *adgf*¯

Given that adenosine levels were elevated in the mutants, we attempted to rescue the large mound size observed in the *adgf* mutants by treating them with the adenosine antagonist, caffeine. Caffeine rescued this early developmental defect in a dose-dependent manner (**Figure 6F**). This suggests that *adgf* may be one of the regulators of group size in *Dictyostelium*. Since the ammonia levels were lower in the mutant, we tested whether exposure to ammonia could rescue the large aggregate size of the *adgf* mutant. Exposing the mutants to 0.01 M ammonia soon after plating or six hours after plating, had no effect on the aggregate size of the mutants (**Figure 6G**), suggesting that while some early effects may be mediated through adenosine receptors, the later effects appear to be independent and likely influenced by ammonia.

Faulty expression of cAMP relay genes in *adgf*¯

cAMP signaling is crucial for tip development and determining cell fate in *Dictyostelium* (Schaap and Wang, 1986; Saxe et al., 1993; Firtel, 1996; Singer et al., 2019). Hence, the expression of genes involved in cAMP relay were measured in WT and *adgf*¯ cells by qRT-PCR. Total cAMP levels and *acaA* gene expression were both low in the *adgf*¯ lines (**Figures 7A** and **7B**). Treating the cells with the pkA activator 8-Br-cAMP or cyclic-di-GMP, the activator of adenyl cyclase (Wang and Schaap, 1985; Chen and Schaap, 2012), reversed the *adgf*¯ mound arrest phenotype (**Figures 7C and D**). Increasing the cyclic-di-GMP dose from 0.5 mM to 1 mM resulted in the formation of multiple tips (**Figure 7E**). These observations further reinforce that the mound arrest phenotype of the *adgf*¯ lines is due to faulty cAMP signaling. Blocking the phosphodiesterase (*pde4*) activity could also lead to higher cAMP levels transiently. When treated with 3-Isobutyl-1-methylxanthine (IBMX), a known PDE4 inhibitor (Bader et al., 2007; Siegert and Weijer, 1989), there was no effect on tip formation in *adgf*¯ mounds (**Figure 7F**), although caffeine restored tip formation (**Figure 7G**). Thus, in spite of impaired expression of cAMP relay genes, the chemotaxis activity is not altered in the mutant.

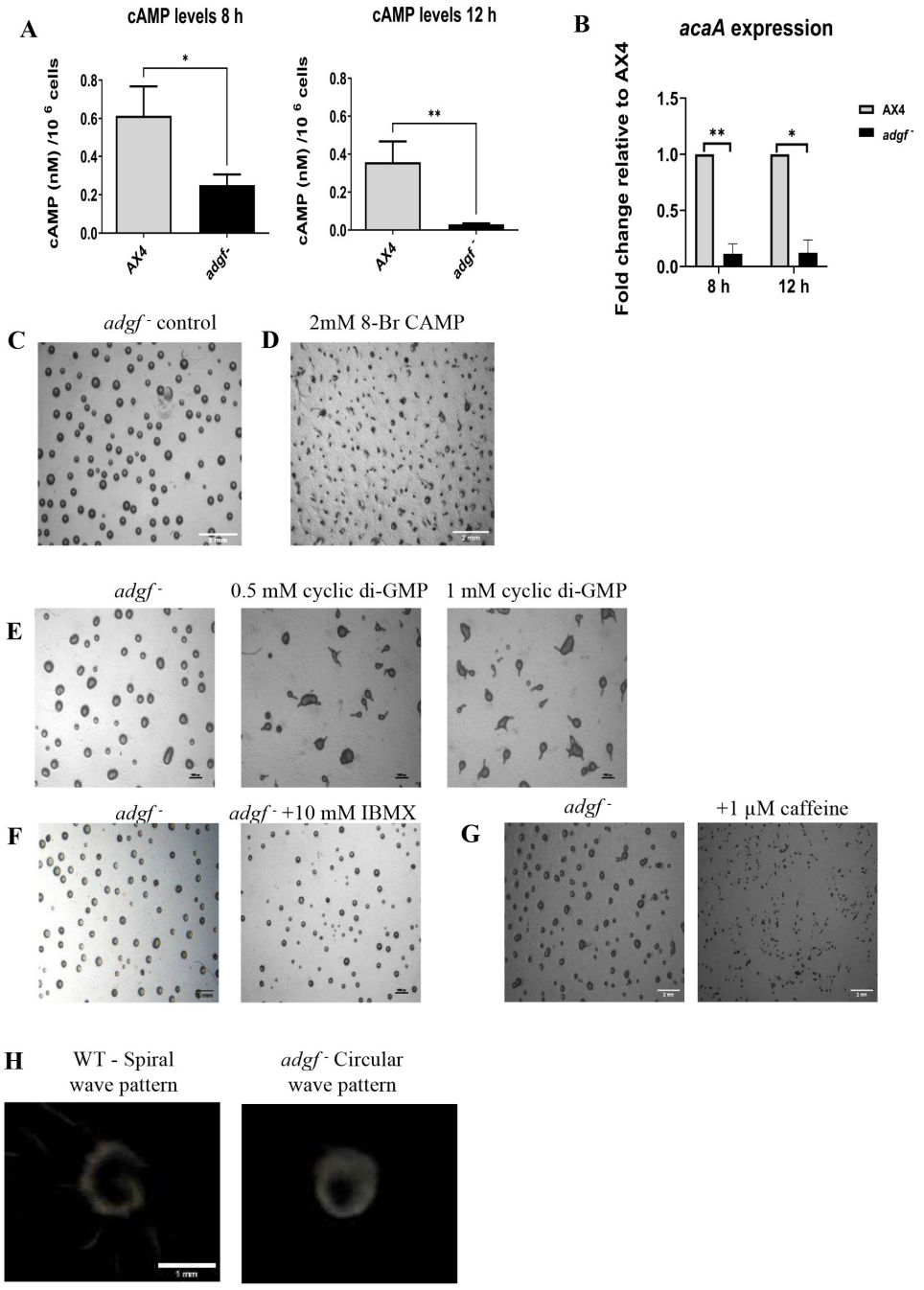

Figure 7.

Impaired cAMP signaling in *adgf*⁻.

A) Total cAMP levels in WT and *adgf*⁻ mounds were quantified using cAMP- XP assay kit (Cell signaling, USA). Level of significance is indicated as *p< 0.05, **p< 0.01; (n=3). **B)** *acaA* expression was quantified using qRT-PCR. The error bars represent the mean ± SEM (n=3). **C)** *adgf*⁻ mounds. **D)** *adgf*⁻ mounds were treated with 2 mM pkA activator 8-Br-cAMP and imaged after 3.5 h. Scale bar: 2 mm; (n=3). **Treatment with cyclic di-GMP and caffeine rescues the mound arrest phenotype. E)** Addition of cyclic-di-GMP restored tip formation in *adgf*⁻ 4 h after the treatment. Scale bar: 1 mm; (n=3). **F)** PDE inhibitor (IBMX) treatment failed to rescue the *adgf*⁻ mound arrest. Scale bar 1 mm; (n=3). **G)** *adgf*⁻ mounds treated with caffeine formed tips 3.5 h post treatment. Scale bar: 2 mm; (n=3). **Altered cAMP wave pattern in *adgf*⁻. H)** Optical density wave images depicting cAMP wave generating centers in WT and *adgf*⁻. WT shows spiral wave pattern and *adgf*⁻ exhibits circular wave propagation.

Circular instead of spiral cAMP waves in *adgf*¯ mounds

Low *acaA* expression, reduced cAMP levels and enhanced cell-cell contacts in *adgf*¯ is likely to impair cAMP wave propagation and to ascertain if this is true, the cAMP signal propagation in WT and *adgf*¯ mounds were compared using dark field optics. In contrast to the WT, which displayed a spiral wave propagating center, the *adgf* mutant exhibited a circular wave propagating center throughout, suggesting that the cAMP relay is impaired (**Figure 7H**; Supplementary videos S3 and S4).

Ammonia restores tip formation by regulating *acaA/pde4* expression

adgf expression peaks at 16 h and to find if *adgf* expression is regulated by the substrate or the product, WT cells treated with different concentrations of adenosine (100 nM, 1 µM, 0.5 mM), were plated on KK2 agar plates and harvested at 16 h for RNA isolation. Independently, WT mounds on KK2 agar plates were exposed to different concentrations of volatile ammonia (0.1 mM, 1 mM, 10 mM) for 3 h and thereafter, the mRNA expression levels of *adgf*, *acaA* and *pde4* were examined. All the rescue experiments involving ammonia is for 3.5 h time period. With 100 nM adenosine, the expression of both *adgf* and *acaA* decreased when compared to controls but at higher adenosine concentrations (1 µM, 0.5 mM), the expression levels of these two genes were comparable to controls (**Figure 8A**). Interestingly, *pde4* expression decreased gradually with increasing adenosine concentrations (100 nM to 0.5 mM), but increased steadily with increasing ammonia levels.

In mounds exposed to 0.1 mM ammonia, the expression of *adgf* decreased but exposure to 1 mM, and 10 mM ammonia, respectively caused a 3 and 2.3-fold upregulation of *acaA* expression. This observation suggests that ammonia may be rescuing the mound arrest phenotype by enhancing *acaA* expression and thus cAMP levels. In similar conditions, a considerable increase in *pde4* expression was observed (**Figure 8B**), which may be necessary for controlling cAMP production in response to NH3 treatment. In conclusion, the expression of *adgf* is influenced both by the substrate adenosine as well as the product ammonia in a dose dependent manner.

adgf¯ cells sort to prestalk in a chimera with WT

To determine if *adgf* favours the differentiation of one cell type over the other, the expression of prestalk (pst) and prespore (psp) markers were examined in the mutant by realtime PCR. While the expression of pst markers, *ecmA* and *ecmB* were significantly upregulated, the psp-specific *pspA* gene showed reduced expression in the mutant (**Figure 8C**), suggesting that WT *adgf* favours psp expression.

To know the cell type preference of the *adgf* mutants in a chimera with WT, a fraction (20%) of any one cell type was labelled with a cell tracker stain DIL and the development was tracked thereafter. In the slugs that formed after reconstituting labelled WT or *adgf*^{OE} cells with 80% unlabelled *adgf*¯ cells, the fluorescence was largely confined in the psp region. Conversely, when *adgf*¯ cells stained with DIL were reconstituted with unlabelled WT or *adgf*^{OE}, the fluorescence was restricted to the pst part of the slug. In the reconstituted slugs, consistently, labelled WT or *adgf*^{OE} cells occupy the psp, whereas the *adgf*¯ cells end up in the pst region (**Figures 9A**, 9B and 9C). Thus, the distribution of cell types in the mound/slug is significantly influenced by *adgf*, as the mutant cells sort out in a mixture with WT cells and differentiate to pst cells.

Further, when stained with the prestalk marker, neutral red (Yamamoto and Takeuchi, 1983), the staining was intense in the pst and ALCs of *adgf*¯ slugs, and such an intense coloration was not apparent in WT especially in the ALCs (Figure S2A). To further investigate if reduced ADA activity

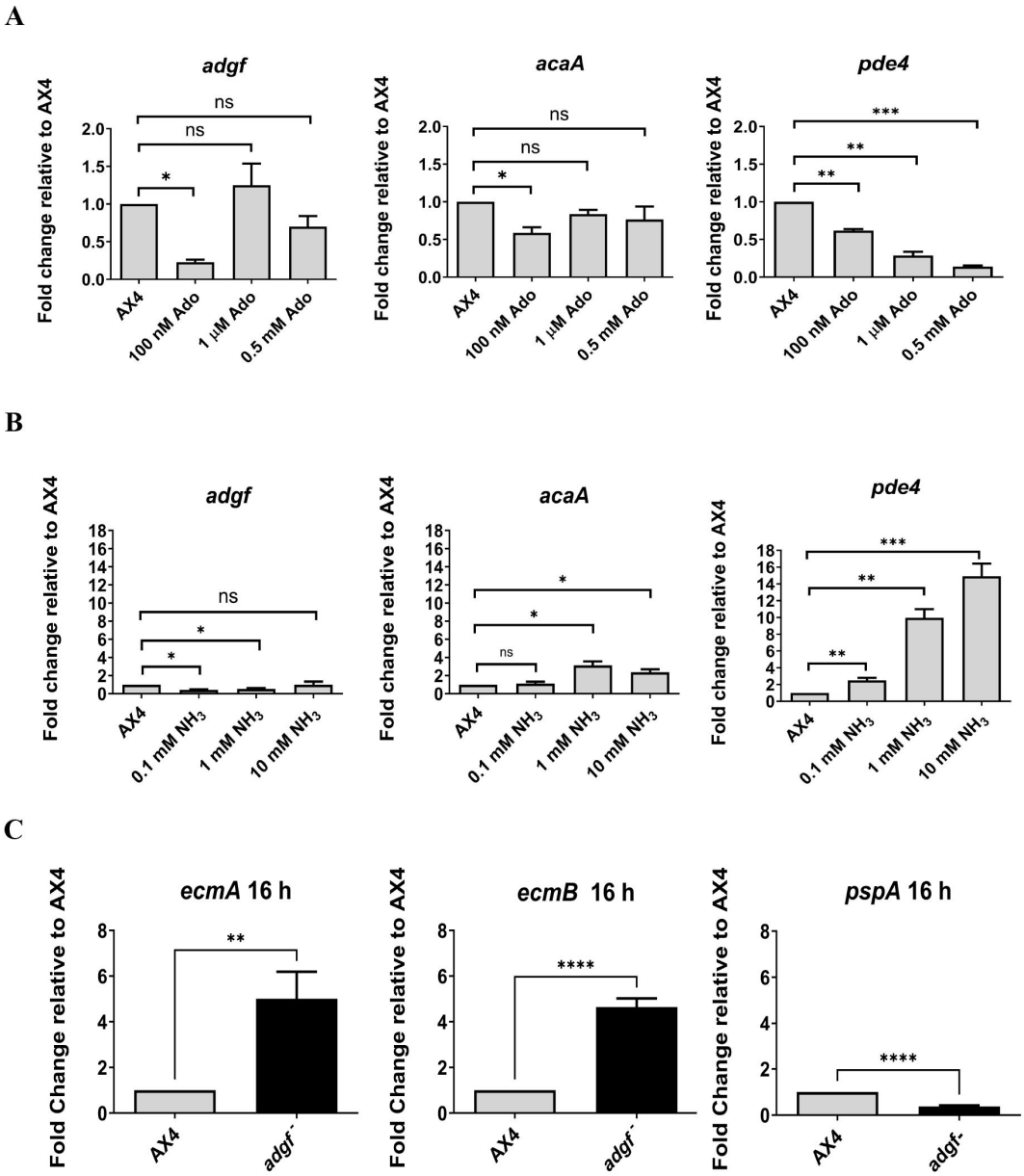

Fig 8.

Expression levels of *adgf*, *acaA* and *pde4* in response to adenosine and ammonia treatment.

A) Expression levels of *adgf, acaA* and *pde4* in response to adenosine treatment (100 nM, 500 nM, 1 µM). **B)** Effect of different concentrations of ammonia (0.1 mM, 1 mM, 10 mM) on the expression levels of *adgf*, *acaA* and *pde4*. Levels of s ignificance i s indicated as * p< 0 . 05 , ** p< 0 . 01 , and *** p< 0 . 001 ; (n=3). **Expression levels of prestalk, *ecmA*, *ecmB* and prespore, *pspA* cell type markers in *adgf*⁻.** The expression profiles of **C)** prestalk (*ecmA*, *ecmB*) and prespore (*pspA*) specific markers in WT and *adgf*⁻ were quantified using qRT-PCR. Level of significance is indicated as *p<0.05, **p<0.01, ***p<0.001 and ****p<0.0001; (n=3). Three independent biological replicates were performed and the error bars represent the mean and SEM. The fold-change in RNA transcript levels is relative to WT at the indicated time points. *rnlA* was used as the internal control (n=3). ns = not significant

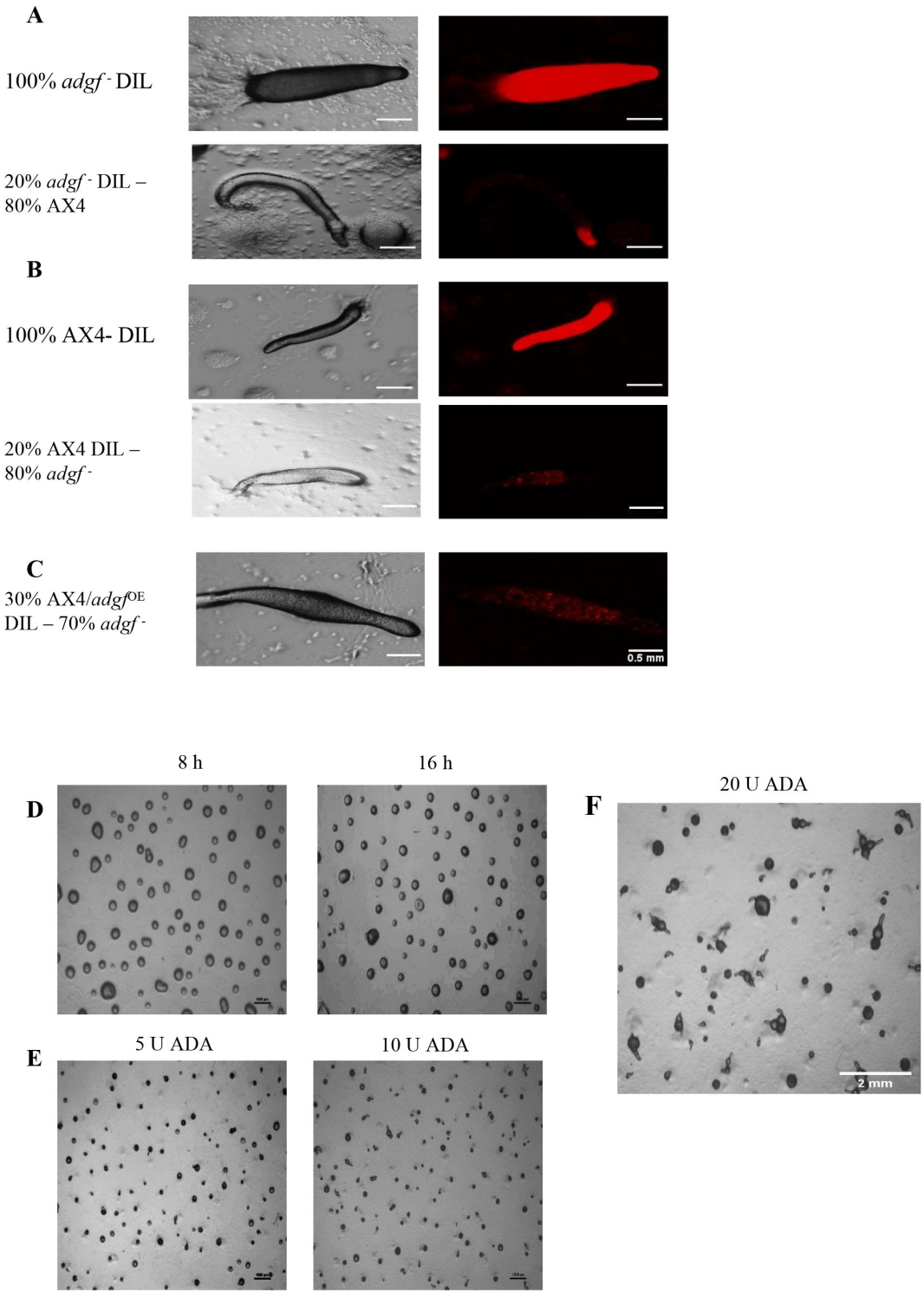

Figure 9.

Reconstitution of WT cells with *adgf*⁻ following DIL staining.

A-C) DIL labelled cells were reconstituted with unlabeled cells and plated for development. Images were captured during the migrating slug stage. The left panel shows bright field, and the right panel shows the corresponding fluorescence images. Scale bar: 0.5 mm; (n=3). ***adgf* acts downstream of histidine kinase *dhkD*. D)** *dhkD* ⁻mutants on KK2 agar plates. **E-F)** 5 U, 10 U or 20 U ADA was added on top of the mounds. Scale bar: 1 mm; (n=3). Images were taken 3.5 h post treatment. Addition of the ADA enzyme rescued the mound arrest phenotype in a dose dependent manner. Scale bar: 2 mm; (n=3).

affects cell type specific marker expression or their pattern in slugs, pst (*ecmA*-GFP, *ecmO*-GFP) or psp (*pspA*-RFP) lines were treated with the ADA inhibitor DCF. While there was no change in pst/psp patterns in the mounds and slugs that formed after a long delay, the *ecmA*- GFP was intense in the tip when compared to WT (Figures S2B). Similar to NR staining pattern in adgf mutant slugs, a prominent expression of *ecmA*-GFP was observed in the ALC region also. Visually, there was no change in *ecmO* or *psp* marker expression in DCF treated slugs (Figures S2C and S2D) suggesting that impaired ADGF activity affects tip specific expression significantly.

adgf acts downstream of the histidine kinase, *dhkD*

In an effort to identify the pathway by which *adgf* acts during tip development, we selected a number of mutant lines with similar mound arrest phenotype such as cAMP receptor B (*carB* $^{-}$), LIM domain containing protein (*limB* $^{-}$), mound mutants (*mndA* $^{-}$) and histidine kinase (*dhkD* $^{-}$) (Saxe et al., 1993; Carrin et al., 1996; Chien et al. 2000; Singleton and Xiong, 2013) and treated the mounds with ADA enzyme. Treatment with 10 U ADA or exposure to ammonia restored tip formation in *dhkD*$^{-}$ mounds and not others tested (Figures S3A and S3C). An increase in ADA concentration (20 U), resulted in the development of multiple tips in *dhkD*$^{-}$ (**Figures 9D**, 9E and 9F). These findings imply that *adgf* acts downstream of *dhkD* in controlling tip development. Similarly, we tested few mutants with multiple tips phenotype, such as tipped mutant (*tipA* $^{-}$), culinB (*culB* $^{-}$), autophagy mutants (*atg7* $^{-}$, *atg8*$^{-}$, and *atg9*$^{-}$) (Stege et al., 1999; Wang and Kuspa, 2002; Otto et al., 2003; Otto et al., 2004, Tung et al., 2010) by adding the ADA inhibitor, DCF (1 mM) to the cell suspension /agar plates and if rescued, those mutants are likely to be in the same pathway controlling tip development. However, DCF treatment had no impact on mutants with multiple tips (Figure S3B).

Impaired expression of other deaminases also results in aberrant tip formation

Several pathways control ammonia levels during development and knockouts in other deaminases (2-aminomuconate deaminase: DDB_G0275081, adenosine monophosphate deaminase: DDB_G0292266, dCTP deaminase: DDB_G0293580, threonine deaminase: DDB_G0277245, N-acetyl glucosamine deaminase: DDB_G0286195, glucosamine-6-phosphate deaminase: DDB_G0278873) show a partial mound arrest phenotype (Figures S4A-F) although the expression of some of these candidates is stronger during development suggesting a prominent and unique role of adenosine deamination in tip development.

High adenosine levels and other related purines do not block tip development

ADA catalyses the conversion of adenosine/deoxy adenosine respectively to inosine/ deoxy inosine. As *adgf* mutants have high adenosine levels, we investigated if the mound arrest could be mimicked in WT by treating with adenosine. Surprisingly, addition of adenosine does not lead to mound arrest in WT (Figure S5A). It is possible that ADA/ADGF converted adenosine analogues to inosine analogues, which in some manner affected development. Hence, WT cells were treated with an adenosine analogue (2'-deoxyadenosine), or guanosine (10 µM each) and they do not cause a mound arrest phenotype either. Similarly, treating *adgf*$^{-}$ mounds with inosine does not restore tip formation (Figures S5B and S5C) suggesting that the blocked tip development is due to faulty adenosine deamination alone.

Cross kingdom rescue of the *adgf* $^{-}$ mound arrest phenotype

Just like WT *Dictyostelum* rescuing the mound arrest phenotype of the mutant, we examined if bacteria physically separated from the mutants would rescue the phenotype. To check this, *Klebsiella aerogenes* and *adgf* mutants were incubated adjacent to each other within a

compartmentalized KK2 agar plate. After 12 h, tip formation was restored in the mutants while in the same time frame, the mounds in controls failed to form tips. Possibly, *Klebsiella* on KK2 with no nutrients would die releasing ammonia restoring tip development in *Dictyostelium* (Figure S6).

Discussion

Dictyostelium ADGF is likely to be secreted growth factor

Multiple sequence alignments, experiments with conditioned media and cell type reconstitution with WT suggests that ADGF is a secreted molecule. AMP deaminase, previously characterized in the mollusk *Helix pomatia*, has been identified as a member of ADGF family (Tzertzinis et al., 2023). It is important to note that ADGF is also known to act on 5'-adenosine monophosphate (AMP) and deoxyadenosine. Studies on the characterization and expression of this growth factor has shown that it is a secreted protein critical for embryonic and larval development in Pacific abalone (Hanif et al., 2022), highlighting the broader role of ADGF in development across species. The human ADA2 enzyme belongs to the novel family of ADGF and crystal structure of ADA2 reveal the presence of a catalytic- and two unique ADA2-specific domains with novel folds, responsible for protein dimerization and interaction with cell surface receptors. Furthermore, the presence of a number of N-glycosylation sites, conserved disulfide bond, and a signal peptide in ADA2 indicate that ADA2 is specifically adapted to function in the extracellular environment (Zavialov et al., 2010).

Possible reasons for increased mound size in the *adgf* mutant

Enhanced cell adhesion influences cohesion and can impact the mound size (Roisin-Bouffay et al., 2000). The cell-cell adhesion genes *cadA* and *csaA* (Coates and Harwood, 2001) were upregulated in the mutant, leading to enhanced adhesion and larger mound size. While over-secretion of *ctn* leads to stream breaking resulting in smaller aggregate formation (Brock and Gomer, 1999), disruption of the *ctn* gene prevents this process, inducing large aggregate formation. *ctn* in turn regulates *smlA* (Brock et al., 2003), impacting the overall aggregate size. Thus, *adgf* mutants have reduced *ctn* and *smlA* expression manifesting large mound formation. Indeed, cells treated with adenosine are known to form large aggregates (Schaap and Wang, 1986) and the first genetic evidence supporting the previous work is from *adgf* mutants, which carry excess extracellular adenosine and form large aggregation streams.

Pathways generating ammonia in *Dictyostelium*

Proteolysis during starvation is believed to be the main source of volatile ammonia in *Dictyostelium* (Hames and Ashworth, 1974; Schindler and Sussman, 1977; White and Sussman, 1961), while RNA degradation is also attributed to yield ammonia during starvation (Walsh and Wright, 1978). During development, amino acids, total protein and RNA levels are reported to reduce with a significant increase in ammonia levels, thus equivocating the source of volatile ammonia (Hames and Ashworth, 1974). Furthermore, several deaminases or enzymatic reactions in *Dictyostelium* may also potentially generate ammonia (Supplementary Table S1). The annotated *D. discoideum* genome contains five evolutionarily conserved family of ammonium transporter/methylammonium permease/rhesus protein (Amt/Mep/Rh) encoding genes (Eichinger et al., 2005), *amtA, amtB, amtC, rhgA,* and *rhgB*, which help in regulating ammonia levels during growth and development. *amtA* and *amtC* antagonistically control developmental processes and are involved in ammonium sensing or transport (Follstaedt et al., 2003; Kirsten et al., 2005; Singleton et al., 2006).

Role of ammonia during *Dictyostelium* development

During early development in *Dictyostelium,* ammonia is known to inhibit aggregation (Schindler and Sussman, 1979; Williams et al., 1984), affect aggregate territory size (Thadani et al., 1977), aggregate density (Feit, 1988), cell fate (Gross et al., 1988), culmination (Davies et al., 1993), and fruiting body size (Lonski, 1976). Ammonia is essential for differentiation in submerged clumps (Sternfeld and David, 1979) and favours prolonged slug migration called 'slugging' over culmination and influences psp over pst differentiation (Newell et al., 1969). Ammonia plays a crucial role in orienting cell masses and accelerating the movement of aggregating cells (Bonner et al., 1986). Enzymatic removal of ammonia causes the quick transition from slug to fruiting thus controlling the morphogenetic pathways (Schindler and Sussman, 1977). By suppressing DIF biosynthesis (Neave et al., 1983), ammonia favors psp over pst development in *Dictyostelium* (Davies et al., 1993; Riley and Barclay, 1990). Further, ammonia prevents the developmental transition of slugs to fruiting bodies (Bradbury and Gross, 1989; Wang and Schaap, 1989). It is interesting to note that ammonia induces tip development (as in *adgf* mutants), but subsequently, tips move away from a source of ammonia. Migration of slugs/ fruiting bodies away from ammonia, reflects a process by which fruiting bodies position themselves from other structures to increase the possibility of spore dispersal (Kosugi and Inouye, 1989). Ammonia by enhancing the collective movement of cells is believed to exert negative chemotaxis (Bonner et al., 1986). Ammonia is known to inhibit tip formation in slugger mutants, but in strains such as NC4 (Gee et al., 1994), ammonia exerts no effect on tip formation as in AX4 (data not shown). The highly acidic, autophagic vesicles in pst cells (Gross, 2009) are believed to catalyze the breakdown of proteins and RNA, also generating ammonia.

ADGF and its substrate, adenosine could serve as a localized source of ammonia. Indeed, cells carrying high ATP, its derivatives cAMP (Bargoda et al., 2009; Singer et al., 2019) and adenosine (Schaap and Wang, 1986), end up in the tip (Hiraoka et al., 2022). Further, 5'- nucleotidase promoter activity is high in pstAB cells (Ubeidat et al., 2002) that significantly covers the tip region suggesting high adenosine levels in the tip. However, extracellular 5'-AMP can be derived from multiple sources such as hydrolysis of cAMP, ATP and RNA (Carpousis et al., 1999).

As a gas, ammonia can diffuse generating a gradient; high in the slug front compared to the posterior. Our results (**Fig. 6A**) also show that the amount of ammonia released from adenosine is in the same order of magnitude as that from other sources (Yoshino et al., 2007). In *adgf* mutants, ammonia levels may not be sufficient enough to neutralize the acidic vesicles and hence, NR staining is intense in the pst region and the ALCs (Bonner, 1952). Thus, excess acidification if not neutralized may lead to mound arrest and if ammonia acts on the acidic vesicles, then, collective migration of cells leading to tip formation may be favoured.

Ammonia is crucial in regulating differentiation, metabolism, and gene expression (Liu et al., 2022, Stein et al., 2013). Ammonium has been shown to induce aberrant blastocyst differentiation, disrupt normal metabolic processes, alter pH regulation, and subsequently affect fetal development in mice (Lane and Gardner, 2003). Newt *Triturus* exposed to ammonia show dorsalization of the ventral marginal zone highlighting the capacity of ammonia to alter embryonic axis formation (Yamada, 1950). Furthermore, research on avian embryos has revealed significant ammonia content in developing eggs, suggesting a potential role for ammonia in the energy metabolism during ontogenesis (Needham, 1926).

Ammonia's effect on cAMP signaling in *Dictyostelium*

Ammonia is known to increase intracellular cAMP levels in *D. discoideum* (Riley and Barclay, 1990; Feit et al., 2001) but Schindler and Sussman, (1977) and Williams et al., (1984) reported that high ammonia levels inhibit the synthesis and release of cAMP. However, some of these experiments use ammonium carbonate (Schindler and Sussman, 1977), or ammonium

chloride (Williams et al., 1984), as a source of ammonia and the possibility of carbonate and chloride ions interfering with development cannot be ruled out. In slugs, ammonia is shown to exert very little effect on cAMP levels (Schaap et al., 1995). In *Dictyostelium mucoroides*, high ammonia levels are known to block the production of extracellular cAMP. The effect of volatile ammonia on aggregation seems to be species specific notably in *P. violaceum, P. pallidum, and D. mucoroides* resulting in wider aggregation territories, while it was not observed in other species such as *D. discoideum* and *D. purpureum* (Bonner and Hoffman, 1963).

Adenylate cyclase (AC) activity is regulated by various factors (Steer, 1975). At physiological levels, ammonium ions increase AC activity in the rat brain by 40% (Yeung et al., 1989), but lowered its activity in the liver by about 30% (Wiechetek et al., 1979). Ammonia has been shown to increase the activity of AC-G in *Dictyostelium* sori (Cotter et al., 1999). High ammonia levels by altering the pH, can affect the activity of numerous enzymes whose activity is pH dependent and thus the activity of AC can be impacted by pH variations. *adgf* mutants with low ammonia levels have reduced cAMP levels and a gradual increase in ammonia, cause a steady but significant increase in *aca*A expression. In other systems (Rat brain), ammonia is known to interact with manganese (Rivera-Mancía et al., 2012; Lu et al., 2020) and this divalent cation is known to increase *aca*A expression in *Dictyostelium* (Loomis et al., 1979; Khachatrian et al., 1987). Possibly, ammonia interacts with metal ions like manganese to form 'ammine complexes' (Lipkowski and Galus, 1973), particularly in aqueous environments or under specific conditions where the appropriate ligands are available and enhances cAMP levels thus rescuing the mound defects of the mutant.

The decision between the formation of the tip (pst cells) and the ALCs are controlled by the tip's production of ammonia, which prevents the migration of ALCs towards the tip (Sternfeld and David, 1982; Feit et al., 1990). Consistent with this observation, our results show that *adgf* mutant lines that have low ammonia levels exhibit enhanced *ecmA* and *ecmB* marker expression. Mutants impaired in DIF-1 synthesis fail to develop pst-O cells in the slug and subsequently also fail to form the basal disc in the fruiting body (Thompson and Kay, 2000). Similar to our observations of cells with high adenosine occupying the tip of the slug, cells with high ATP (that degrades to adenosine) levels, also end up in the centre of the tip (Hiraoka et al., 2022).

Tip organizer development in *Dictyostelium* depends on the differentiation and appropriate sorting of pst and psp cells (Kay et al., 1978; Williams et al., 1989; Saxe et al., 1993; Williams, 2006), a process that relies on signaling of different morphogens including cAMP, adenosine, DIF and ammonia (Bloom and Kay, Williams, 1988; 1988; Riley and Barclay, 1990; Gross et al., 1994; 2006). These morphogens modify one another's effects, and determine the choice of the differentiation pathway as well as the spatial arrangement of cells (Bloom and Kay, 1988). Thus, the rescue of the *adgf* mutant upon exposure to ammonia is likely due to cAMP signaling and cell-cell contact.

Possible reasons for reduced cAMP levels in the *adgf* mutant

The increased expression of PDE's (intra and extracellular) and reduced ACA expression could well explain the lower cAMP levels in the mutant. ADA significantly regulates adenosine levels, thus reducing the activation of adenosine-mediated receptors (Van Haastert, 1983). Two classes of adenosine receptors including adenosine alpha- and beta-receptors are known to be expressed in *Dictyostelium* (Theibert and Devreotes, 1984). When adenosine concentrations are high, beta-receptors bound with adenosine inhibit the binding of cAMP to its receptors, thereby inhibiting cAMP signaling (Newell, 1982; Van Haastert, 1983; Theibert and Devreotes, 1984). High adenosine levels in the *adgf* mutant may also reduce cAMP levels via a similar mechanism.

adgf activity is likely to be different between pst and psp cells as reconstitution with different cell types shows that cells with low adenosine and high ammonia levels end up in psp while cells with excess adenosine and low ammonia attain pst cell fate. Cell death also results in

adenosine/ammonia formation and thus *adgf* activity is likely to be higher in pst than psp to maintain low extracellular adenosine. The mound/slug tip is believed to carry high adenosine levels restricting additional tip formation favouring lateral inhibition (Wang and Schaap, 1985) and our results also show that *adgf*$^{-}$ cells with high adenosine goes to pst than the psp region.

Distorted cAMP waves in mutant

Collective cell movement within mounds is essential for cell sorting and the progression from mounds to finger structures (Kellerman and McNally, 1999). In WT mounds, cAMP waves propagate in a spiral pattern, while in mutants, waves propagate in a concentric circular pattern. Initially, cAMP waves appear as concentric circles that, upon symmetry breaking, form spiral waves (Siegert and Weijer, 1995). With successive wave propagation, the circular ring distorts, and one end curls toward the pulsatile center, creating a spiral wave around the organizing center. In *adgf* mutants, however, defective cAMP relay prevents this transition, likely due to lower cAMP levels. A surge in phosphodiesterase inhibition is thought to regulate this shift from concentric to spiral wave propagation (Palsson and Cox, 1996).

The mound/slug tip of *Dictyostelium* generates cAMP pulses (Traynor et al., 1992), and is known to suppress additional tip formation (Farnsworth, 1973). Adenosine, that inhibits tip formation represses *pde4* expression whereas ammonia, that promotes tip elongation, increases *pde4* expression. Thus, the restoration of cAMP signaling and spiral wave propagation possibly leads to the rescue of the *adgf*$^{-}$ mound arrest phenotype. Surprisingly adenosine exerts little effect on tip development in WT cells and studies of Inouye (1989) also reinforce our observations, showing that adenosine does not significantly influence the conversion of pst to psp cells in shaking culture conditions.

Adenosine deamination drives tip organizer development

A crucial evidence supporting that adenosine deamination is singularly responsible for the rescue of mound arrest comes from experiments where partitioned dish with buffered solution containing adenosine on one side and the mutants on the other half of the dish. Addition of ADA enzyme (10 U) to the buffered solution with adenosine fully restored the tipped mound formation in the other half of the dish. Although ammonia's role in *Dictyostelium* development is well established, this report is the first to show a novel role of ammonia in tip development. If natural variants of *Dictyostelium* with no tips exist in soil, there is a likelihood that they will form fruiting bodies when WT Dictyostelids are nearby. It is important to note that development of an organism in its natural habitat is strongly influenced by volatiles nearby (Schulz-Bohm et al., 2017).

ADA in organizer development and gastrulation in vertebrates

ada/adgf expression is found to be significantly high during gastrulation stages (Figure S7) in several vertebrates (Pijuan-Sala et al., 2019; Tyser et al., 2021) and the process of gastrulation in higher organisms and collective cell movement within the *Dictyostelium* mound are remarkably similar (Weijer, 2009), suggesting an overlooked role of ammonia in organizer development. It is likely that ADA plays a conserved, fundamental role in regulating morphogenesis in *Dictyostelium* and other organisms including vertebrates. The human homologue of *adgf*, CECR1, is a potential gene for the genetic disorder, Cat-eye syndrome and thus, *Dictyostelium* may also serve as a model to study this condition.

dhkD functions upstream of *adgf*

The histidine kinase *dhkD*, a member of the two-component family of histidine kinases, appears to function upstream of *adgf*, adding to our understanding of the signaling cascade in *Dictyostelium*. Histidine kinases play essential roles in regulating developmental transitions, with *dhkC*, for example, initiating the late developmental program that ultimately leads to fruiting body formation (Singleton et al., 1998). This function of *dhkC* is regulated in part by ammonia levels,

as low ammonia concentrations have been shown to inhibit the *dhkC* phospho-relay, thereby influencing developmental outcomes (Kirsten et al., 2005). In *Dictyostelium*, several histidine kinases, including *dhkA*, *dhkB*, *dhkC*, and *dokA*, coordinate cAMP signaling to modulate the activity of PKA, a cAMP-dependent protein kinase that is essential for proper development (Anjard and Loomis, 2003). These findings suggest the interdependencies within the signaling network in regulating multicellular development in *Dictyostelium*.

Model of ADGF action

High extracellular cAMP at the slug front (Singer et al., 2019) is expected to generate high adenosine, which however could arise from other sources and thus ammonia levels are expected to be higher in the slug front compared to the back. Possibly, ammonia generated extracellularly is quenched rapidly by the intracellular acidic compartments of pst cells, increasing its pH and favouring collective cell movement driving mound/ slug tip development. It is important to note that ammonia is known to promote psp than pst differentiation. Although ammonia is likely to be formed from several sources in *Dictyostelium*, a critical threshold concentration of ammonia may be necessary for tip development. The failure of even one pathway may result in a drop-in ammonia levels, exerting an effect on development (**Figure 10**). Overexpression of *ecmA* and downregulation of *pspA* (as measured by realtime PCR) in the mutant suggests that there is a change in cell type differentiation as suggested by the sorting experiments. This could suggest that the differentiation of the cells is blocked at an early prestalk cell fate. Thus, ammonia is likely to be important for the maturation of tip cells.

Our study shows that *adgf* acts downstream of *dhkD* and *in silico* studies have shown that *dhkD* interacts with *adgf* (Figure S8A). Therefore, it is likely that in the presence of ammonia, *dhkD* activates the phosphorelay, in turn increasing intracellular cAMP levels, leading to tip formation. Histidine kinase *dhkC* is known to phosphorylate *regA* in *Dictyostelium* (Thomason et al.,1999). However, based on docking we found no direct interaction of *regA* with ADGF (data not shown). Thus, the integration of cytokinin and histidine kinase signaling ensures coordinated multicellular organization in *Dictyostelium* (Aoki et al., 2020). Previous work in other systems have found ADA to be interacting with CD 26 (dpp IV) (Tanaka, 1993) and docking DdADGF with AprA (dpp8) (Figure S8B) also support the observations. However, adding ADA inhibitor to *aprA* mutant (dpp8), show no effect on the phenotype (data not shown).

Organisms from different kingdoms often interact in complex ways such as symbiosis, predation, competition etc., which can have significant effects on ecosystem dynamics (Helgason et al., 1998; Harrison, 2005). Such interactions are often mediated through volatiles affecting the physiology of each other just like the bacterial volatiles affecting the development of *Dictyostelium.* However, it needs to be ascertained if this particular volatile is ammonia.

Supplementary Results

Genes involved in autophagy and tipped mound formation do not show altered expression in the mutant

Autophagy helps maintain cellular homeostasis by promoting the breakdown of damaged proteins and organelles (Mizushima et al., 2008), and ammonia is recognised to be a diffusible regulator of autophagy in human cells (Eng et al., 2010). To investigate if autophagy is impaired in the mutant, the expression of autophagy markers *atg8* and *atg18* were examined and there was no discernible change in the expression levels when compared to WT (Figure S9A). The tipless to tipped mound transition as well as late developmental gene expression is regulated by *gbf*A, a G-box binding factor (GBF). However, in the *adgf* mutant the *gbf*A expression levels were

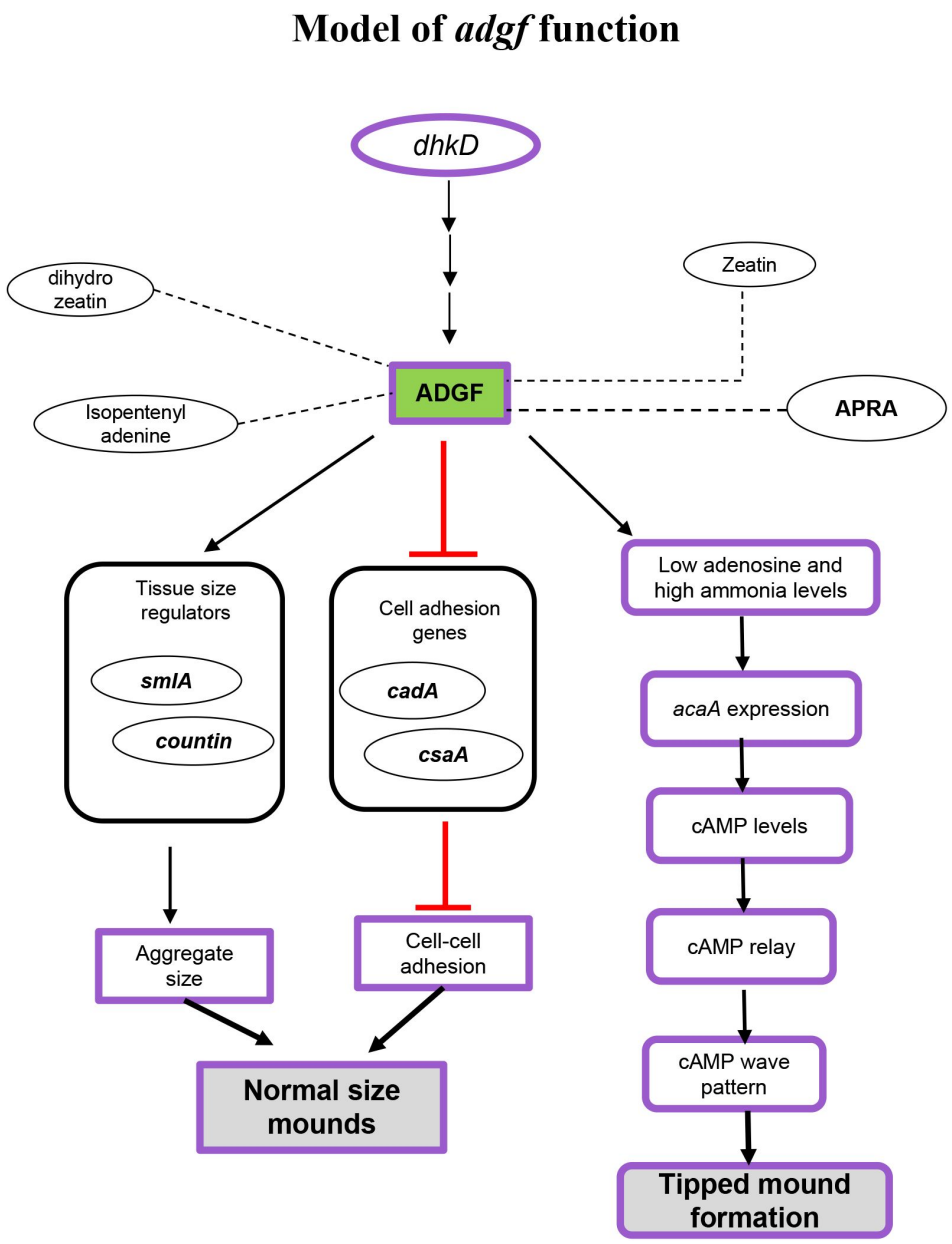

Fig 10.

Model illustrating the role of *adgf* in development *adgf* supresses the expression of genes involved in cell adhesion, *cadA and csaA*.

adgf regulates aggregate size and tip development by directly acting on adenosine, ammonia levels and cAMP signaling. Line ending in an arrow implies that the previous gene/factor either directly or indirectly raises the activity or levels of the second; line ending in a cross-bar indicates inhibition. Dotted lines indicate ADGF interacting with APRA, and the cytokinins zeatin, dihydro zeatin and isopentenyl adenine.

comparable with no significant difference between the WT at 16 h (Figure S9B). Without the assay for autophagy as well as assay for GBF activity, these expression studies alone are not conclusive to rule out the role of these factors in tip formation.

ADA does not deaminate cytokinin

ADA is known to interact with 5'AMP (Hanif et al., 2022) and in *Dictyostelium*, 5'-AMP serves as a direct precursor of cytokinin, playing a significant role in cellular signaling and development (Taya et al., 1978). Although docking studies suggest that binding of ADGF with cytokinins (zeatin, dihydrozeatin, isopentenyl adenine) is moderate, (data not shown), we carried a functional assay by mixing cytokinin and ADA with KK2 buffer in one side of the Petridish and found no rescue of the mutant (Figure S10) in such conditions suggesting no functional activity between ADA and cytokinin.

Supplementary discussion

Plausible routes of caffeine action rescuing the mound arrest phenotype

The *adgf* mound arrest could be rescued by the addition of the adenosine antagonist, caffeine but treatment with the *pde4* inhibitor, IBMX failed to rescue the mound arrest. Caffeine is known to reduce adenosine levels in blood plasma (Conlay et al., 1988) and also increase ammonium levels in urine samples of rabbits (Bernheim and Bernheim, 1945). Thus, the mound rescue upon caffeine treatment may be a result of reduced adenosine and increased ammonia levels. With respect to caffeine action on cAMP levels, the reports are contradictory. Caffeine has been reported to increase adenylate cyclase expression thereby increasing cAMP levels (Hagmann, 1986) whereas Alvarez-Curto et al., (2007) found that caffeine reduced intracellular cAMP levels in *Dictyostelium*. Although, caffeine is moderately potent in inhibiting PDE enzyme activity, the *in vivo* concentrations are likely to be low to be associated with effective PDE inhibition (Burg and Werner, 1975; Daly, 1993).

Material and Methods Bioinformatic analyses of ADGF

The genomic sequence and the protein sequence of ADGF were obtained either from dictybase (*http://dictybase.org*) or NCBI database (*https://www.ncbi.nlm.nih.gov/*). Within the *Dictyostelium* ADGF, the ADA domain was identified by SMART and BLAST (*http://smart.embl-heidelberg.de/*) (*https://blast.ncbi.nlm.nih.gov/Blast.cgi*) (Altschul et al., 1990; Letunic and Bork, 2018) analyses. A phylogenetic tree was generated by aligning multiple amino acid sequences of ADGF from several taxa. Neighbour Joining approach and the MUSCLE alignment tool of the MEGAX programme were used for constructing the tree (Saitou and Nei, 1987). The tertiary structure of ADGF was obtained using the online programme alphafold (*https://alphafold.ebi.ac.uk/*) (Jumper et al., 2021), and PyMol was used for viewing the images. The expression profiles of *ada* and *ada2* during mouse and human gastrula development were retrieved from the marionilab.cruk.cam.ac.uk/MouseGastrulation2018/ and human-gastrula.net/ databases (Pijuan-Sala et al., 2019; Tyser et al., 2021), respectively. Protein-protein docking was carried out using High Ambiguity Driven Protein-Protein Docking (HADOCK) version 2.4.

Culture and development of *Dictyostelium discoideum*

D. discoideum (WT-AX4) cells or the mutant *adgf* derived from AX4, (DBS0237637) were cultured in modified maltose-HL5 medium (Formedium, UK) with 100,000 U/L penicillin and 0.1 g/L streptomycin. Three independent insertional mutants (GWDI_17_D_7, GWDI_47_C_1, GWDI_132_H_3) in the *adgf* gene (insertion in exon 2 in all three mutants) were obtained from the GWDI bank (*https://remi-seq.org*), in *Dictyostelium* stock centre, North Western University, USA

(Gruenheit et al., 2021). The mound defects were identical in all three and GWDI_47_C_1 alone was characterised further. The culture was raised as a monolayer in Petri plates or grown in an Erlenmeyer flask in shaking conditions at 150 rpm and 22 °C, to a cell density of 2-4x10^6 cells/ml. The cells were also grown on SM/5 agar plates supplemented with *Klebsiella aerogenes* at 22 °C (2 g/L glucose, 2 g/L protease peptone, 0.4 g/L yeast extract, 1 g/L MgSO4.H2O, 0.66 g/L K2HPO4, 2.225 g/L KH2PO4, 1% Bactoagar, pH 6.4). For developmental assays, freshly starved cells were washed twice with ice cold KK2 buffer (2.25 g KH2PO4 and 0.67 g K2HPO4 per litre, pH 6.4), and plated on 1% non-nutrient KK2 agar plates at a density of 5x10^5 cells/cm^2 (Nassir et al., 2019). Thereafter, the plates were incubated in dark conditions at 22 °C for development.

Dictyostelium genomic DNA isolation

WT and *adgf*$^-$ cells grown axenically were harvested, and the pellet was resuspended in 1 ml of lysis buffer (50 mM Tris-Cl, pH 8; 10 mM EDTA; 0.8% SDS). To this mixture, 200 µl of Nonidet P-40 (NP40), a non-ionic detergent, was added, vortexed and centrifuged at 12,000 g for 15 min at room temperature (RT). The resultant pellet was gently vortexed, resuspended in 500 µl of lysis solution containing 200 µg/ml Proteinase K, and incubated at 65 °C for 30 min. 300 µl of phenol: chloroform was added to this suspension, centrifuged at 18,000 g for 10 min at RT, and the resultant aqueous phase was extracted carefully. An equal amount of chloroform was added and centrifuged at 18,000 g for 10 min at RT. Following this, 750 µl of pure ethanol was added to the suspension, which was then centrifuged at 12,000 g for 15 min at 4 °C. Genomic DNA was precipitated by adding twice the volume of absolute ethanol and 1/10^{th} the volume of 3 M sodium acetate. After a 10 min centrifugation at 15,000 g, the pellet was cleaned using 70% ethanol and stored at 4 °C. Electrophoresis was conducted in TAE buffer at 50 V using a Medox power pack system (India), and the integrity of DNA was confirmed on a 1% agarose gel.

Validation of the *adgf* mutant

To validate the blasticidin (*bsr*) cassette insertion in the adgf mutant, WT and *adgf*$^-$ genomic DNA were isolated, and a diagnostic PCR was performed using the gene and *bsr* insert specific primers in accordance with the guidelines provided in the GWDI website. A qRT-PCR was carried out to confirm the absence of *adgf* expression in the mutant cells. The primers used for mutant validation are listed in Supplementary Table S2.

Quantitative real-time PCR (qRT-PCR)

Total RNA was extracted from WT and *adgf*$^-$ cells using Trizol reagent (Favorgen, USA) at specified intervals (every four hours from 0 to 24 h). cDNA was synthesized from the total RNA using a PrimeScript 1st Strand cDNA Synthesis Kit (Takara, Japan). Random primers from the manufacturer were used to generate the cDNA from a template of 1 µg total RNA. qRT-PCR was performed using SYBR Green Master Mix (Thermo Scientific, USA) and 1 µl of cDNA. The expression levels of *adgf*, *acaA*, cAMP receptor A (*carA*), phosphodiesterases (*pdsA*, *regA*), 5' nucleotidase (*5'nt*), extracellular matrix A (*ecmA*), extracellular matrix B (*ecmB*), prespore A (*pspA*), countin (*ctn*), and small aggregate (*smlA*) were quantified with a QuantStudio Flex 7 (Applied Biosystems, USA). The mitochondrial large RNA subunit (*rnlA*) served as an internal control. qRT-PCR data analysis was conducted according to the method described by Schmittgen and Livak (2008). The primer sequences used for qRT-PCR are provided in Supplementary Table S4.

Generation of *adgf* over expression construct

The full-length 1.7 kb *adgf* sequence was PCR-amplified using ExTaq polymerase (Takara, Japan) with WT genomic DNA as the template. The amplified product was then ligated into the pDXA-GFP2 vector at the HindIII and KpnI restriction sites. Both *adgf*$^-$ and WT cells were electroporated

with this vector, and G418-resistant clones (10 µg/ml) were isolated for further analysis. The expression of *adgf* was confirmed by semi-quantitative PCR. The corresponding primer sequences are listed in Supplementary Table S3.

Transformation of Dictyostelium discoideum

WT and *adgf*$^-$ cells grown axenically were harvested, washed twice with ice-cold EP buffer (10 mM KH2PO4, 10 mM K2HPO4, 50 mM sucrose, pH 6.2), and resuspended in 100 µl of EP++ solution (10 K2HPO4 mM, 10 mM KH2PO4, 50 mM sucrose, 1 mM MgSO4, 1 mM NaHCO3, 1 mM ATP, 1 µM CaCl2) containing 10 µg of plasmid vector (Nassir et al., 2019) in pre-cooled cuvettes (BioRad, USA). The cells were electroporated using a BTX ECM830 electroporator (Harvard Apparatus, USA) at 300 V with 2 ms pulses and five square wave pulses at 5-second intervals. The cells were then transferred to a Petri dish with 10 ml of HL5 medium and incubated at 22 °C. After 24 hours, G418 (10 µg/ml) was added to the medium, and resistant colonies were selected for further analysis.

Preparation of conditioned media (CM)

WT and *adgf*$^-$ cells grown in HL5 medium were collected at the mid-log (ML) phase, resuspended in KK2 buffer at a density of $1x10^7$ cells/ml, and incubated at 22 °C with shaking for 20 hours. The clarified supernatant obtained after centrifugation was used for the experiments.

Assay for ADA activity

The total ADA activity from *Dictyostelium* was determined as per the protocol of the manufacturer (Abcam, USA; Cat No: ab204695). For sample preparation, $5x10^5$ cells/cm^2 were seeded onto KK2 agar plates and at the mound stage, ice cold ADA assay buffer was flooded, then vigorously pipetted to disrupt the mound integrity. The cell homogenate was agitated on a rotary shaker at 4 °C for 15 min and then centrifuged at 12,000 rpm for 10 min in a cold microfuge tube. The supernatant was subjected to the ADA assay. This ADA test detects inosine, generated from adenosine break down through a multi-step reaction. The intermediate formed combines with the probe to produce uric acid, which is quantified at OD 293 nm. BCA (Bicinchonic acid) assay kit (Thermoscientific, USA) was used for determining the protein concentration. One unit of ADA activity is defined as the amount of enzyme that hydrolyses adenosine to yield 1 µmol of inosine per min under the assay conditions.

Adenosine quantification

Total adenosine levels from *Dictyostelium* mounds were measured according to the protocol using the Adenosine Assay Kit (Abcam, USA; Cat No: ab211094). Cells grown in HL5 were collected, washed and plated on KK2 agar plates. The lysis buffer was added to the plates with mounds and mixed thoroughly. 50 µl of the lysate was mixed with 2 U of ADA and was subjected to incubation for 15 min at RT. Adenosine quantification involves the use of ADA and after a series of enzymatic reactions, an intermediate is formed which reacts with the adenosine probe generating a fluorescent product. Using a spectrofluorometer (Perkin Emer, USA; λEx = 544 nm/λEm = 590), the fluorescence intensity can be measured which is proportional to the concentration of adenosine (Perkin Emer, USA; λEx = 544 nm/λEm = 590). The adenosine levels were quantified using the adenosine standard curve.

Quantification of ammonia

Ammonia assay kit (Sigma-Aldrich, USA; Cat No: AA0100) was used for estimating the total ammonia levels. WT and *adgf*$^-$ cells developed on KK2 agar plates were sealed with parafilm and incubated at 22 °C. The mounds were collected using lysis solution, and the debris was removed by centrifugation at 10,000 g for 10 min. The supernatant was used for further analysis. For the ammonia assay, 1 ml of assay reagent was mixed thoroughly with either 100 µl of samples or standards, incubated for 5 min at RT, and the absorbance was measured at 340 nm. Then, 10 µl of

L-glutamate dehydrogenase (GDH) solution was added to each cuvette, and after a 5-min incubation at 25 °C, the absorbance was measured again at 340 nm using a spectrophotometer (Eppendorf, Germany). In the presence of GDH, ammonia combines with α- ketoglutaric acid and reduced NADPH to produce L-glutamate and oxidised NADP+. The decrease in absorbance at 340 nm is proportional to the ammonia concentration. The ammonia standard curve was used to calculate the ammonia levels.

Volatile ammonia generation

To generate ammonia, 1 ml of 1 N NaOH and 1 ml of NH4Cl (concentrations used 0.1 mM, 1 mM, 10 mM) were mixed thoroughly (Thadani et al., 1977; Feit et al., 1990) and from this mix, 2 ml was aliquoted in the upper half of the Petri dish. The other half of the plate with the *adgf*$^{-}$ mounds on KK2 agar were inverted, sealed and incubated at 22 °C. To determine whether WT mounds, physically separated from the mutants could rescue the mound arrest, WT (1x10^{6} cells/cm^{2}) and *adgf*$^{-}$ (5x10^{5} cells/cm^{2}) cells were developed on KK2 agar plates on either side of compartmentalised and sealed Petri plates. *adgf*$^{-}$ cells developed on either side of the dish served as controls.

Quantification of cAMP

Using the cAMP-XP test kit and following the manufacturer's instructions, total cAMP levels were determined from both the WT and the mutant (Cell signaling, USA). WT and *adgf*$^{-}$ mounds were disrupted and collected in 1 ml ice cold KK2 buffer. After centrifuging the pellet, 100 µl of 1X lysis solution was added, and the mixture was allowed to rest on ice for 10 min. Following that, 50 µl of lysate and 50 µl of HRP-conjugated cAMP solution were added to the test plates, which were then shaken horizontally at RT. After a 3-hour incubation, the wells were emptied and washed three times with 200 µl of 1X wash buffer. 100 µl of stop solution was added to halt the reaction, and the absorbance was measured at 450 nm using a spectrophotometer (Biorad, USA). The cAMP standard curve was used to determine the cAMP levels.

Visualisation of cAMP waves using dark field optics

5x10^{5} cells/cm^{2} were developed on KK2 agar plates under moist, dark conditions to monitor the propagation of the cAMP wave. Using a Nikon DS-5MC camera mounted on a Nikon SMZ- 1000 stereo zoom microscope, a time-lapse video of the aggregation was captured in real-time (Nikon, Japan). cAMP optical density waves were displayed by subtracting the image pairs (Siegert and Weijer, 1995) after processing the images with the NIS-Elements D program or ImageJ (NIH, USA).

Under agarose cAMP chemotaxis assay

The under-agarose cAMP chemotaxis assay (Woznica and Knecht, 2006; Singh and Insall, 2022) was carried out with cells obtained from WT and *adgf*$^{-}$ mounds. Briefly, the cells were starved in KK2 buffer at 1x10^{7} cells/ml density. Three parallel troughs, each measuring 2 mm in width, were set up on a Petri dish containing 1% agarose. In the outer two troughs, 100 µl of WT and *adgf*$^{-}$ cell suspension was aliquoted respectively and 10 µM cAMP was added to the central trough. Cell migration toward cAMP was recorded every 30 s over a total duration of 20 min using the NIS-Elements D software and an inverted Nikon Eclipse TE2000 microscope (Nikon, Japan). 35 cells were tracked each time and subsequently analysed using ImageJ (NIH, USA).

Reconstitution of WT with mutant cells

WT and *adgf*$^{-}$ cells cultured in HL5 medium, were harvested at the ML phase by centrifugation, rinsed twice with ice-cold KK2 buffer. The cells mixed in different ratios (1:9, 2:8 and 1:1) were adjusted to a final density of 5x10^{5} cells/cm^{2}, plated on 1% KK2 agar plates, and incubated at 22 °C for development.

Tracking cell fate after reconstitution

Dictyostelium cells harvested from fresh HL5 media were resuspended at a density of $1x10^6$ cells/ml in KK2 buffer, followed by incubation at 22°C for 1.5 h in shaking conditions with 0.2 µM DIL, (1,1'-Dioctadecyl-3,3,3',3'-Tetramethylindocarbocyanine Perchlorate, Invitrogen, USA) a cell tracker dye. DIL has been used extensively as a cell tracker in *C. elegans*, *Xenopus and* mice (Schultz and Gumienny, 2012; Xu et al., 2020; Erdogan et al., 2016). WT or *adgf*¯ cells labelled with DIL were reconstituted with the unlabelled cells in a ratio of 1:9, 2:8 and 1:1 and plated for development. In the ratios mentioned, the smaller fraction represents the stained cells. DIL is a lipophilic dye that selectively stains the plasma membranes of living cells, allowing visualization and analysis of cell morphology.

Neutral red staining of mounds and slugs

WT and *adgf*¯ cells harvested from HL5 cultures were resuspended at a density of $1x10^7$ cells per ml in KK2 buffer and treated with 0.005% neutral red (NR) solution for 15 min at RT in shaking conditions (Bonner, 1952). The stained cells were washed twice with KK2 buffer, plated in buffered agar plates and thereafter, NR stained slugs were observed using an upright microscope.

Cell-cell adhesion assay

After 14 h of development on phosphate buffered agar plates, WT and *adgf*¯ mounds were disaggregated by repeated pipetting and vortexing using ice-cold KK2 buffer. Dissociated cells were resuspended in KK2 buffer and incubated at 150 rpm for 45 min. Single and non-adherent cells were counted using a Neubauer chamber (Lam et al., 1981).

Treatment of *Dictyostelium* cells with different compounds

A highly specific ADA inhibitor, DCF that inhibits both extra and intra-cellular ADAs (Cha et al., 1975) was mixed with the WT cell suspension and plated on 1% non- nutrient KK2 agar plates at a density of $5x10^5$ cells/cm^2. Of the different DCF concentrations tested (10 nM, 50 nM, 100 nM and 1 µM), 100 nM showed complete tip inhibition.

For the enzymatic rescue assay, 10 U of bovine ADA dissolved in KK2 buffer (Sigma-Aldrich, USA) was added onto mutant mounds. The concentrations of 8-Br-cAMP (2 mM), cAMP (0.1 mM, 0.5 mM), c-di-GMP (0.1 mM, 0.5 mM), adenosine (1 µM, 10 µM, 100 µM, 1 mM), caffeine (10 nM, 100 nM, 1 µM) and IBMX (3-isobutyl-1-methylxanthine 0.5 mM) were based on previous publications (Chen et al., 2017; Chen and Schaap, 2012; Nassir et al., 2019; Siegert and Weijer, 1989) and these compounds were added independently either on top of the mounds or supplemented while plating. All the fine chemicals were from Sigma-Aldrich, USA except when mentioned.

Microscopy

Microscopy was performed using a Nikon SMZ-1000 stereo zoom microscope with epifluorescence optics, Nikon 80i Eclipse upright microscope, or a Nikon Eclipse TE2000 inverted microscope, connected with a digital sight DS-5MC camera (Nikon). Image processing was carried out using NIS-Elements D (Nikon) or Image J.

Statistical tools

Data analyses were carried out using Microsoft Excel (2016). Statistical significance was determined by paired or unpaired, one-tailed Student's t-test (GraphPad Prism, version 6).

Acknowledgements

We gratefully acknowledge the help of NBRP Nenkin, Japan and *Dictyostelium* Stock Center (DSC), Northwestern University, USA for providing various strains and plasmids used in this study. We thank Prof. Richard Gomer, Texas A&M, USA for providing *aprA* mutant strain. We thank Prof. Kei Inouye, Kyoto University, Japan and Prof. Kees Weijer, University of Dundee, UK for their comments on an earlier version of the manuscript.

Additional information

Author contributions

P.H. and R.B. conceptualized the work. P.H. performed all experiments. P.H. and R.B. analysed the data and wrote the manuscript.

Additional files

Supplementary file

Supplementary videos

References

1. Aoki M. M., Emery R. J., Anjard C., Brunetti C. R., Huber R. J 2020) **Cytokinins in Dictyostelia–A unique model for studying the functions of signaling agents from species to kingdoms** *Frontiers in Cell and Developmental Biology* **511**

2. Altschul S. F., Gish W., Miller W., Myers E. W., Lipman D. J 1990) **Basic local alignment search tool** *J. Mol. Biol* **215**:403–410

3. Alvarez-Curto E., Weening K. E., Schaap P 2007) **Pharmacological profiling of the Dictyostelium adenylate cyclases ACA, ACB and ACG** *Biochemical Journal* **401**:309–316

4. Anjard C., Loomis W. F, Inouye M, Dutta R 2003) **Histidine kinases of Dictyostelium** *Histidine Kinases in Signal Transduction* Academic Press :421–438

5. Annesley S. J., Fisher P. R 2009) **Dictyostelium discoideum—a model for many reasons** *Molecular and Cellular Biochemistry* **329**:73–91

6. Bader S., Kortholt A., Van Haastert P. J. 2007) **Seven Dictyostelium discoideum phosphodiesterases degrade three pools of cAMP and cGMP** *Biochemical Journal* **402**:153–161

7. Bagorda A., Das S., Rericha E. C., Chen D., Davidson J., Parent C. A 2009) **Real-time measurements of cAMP production in live Dictyostelium cells** *Journal of Cell Science* **122**:3907–3914

8. Bernheim F., Bernheim M. L 1945) **Note on the effect of caffeine on ammonia and urea excretion in rabbits** *American Journal of Physiology-Legacy Content* **145**:115–117

9. Bloom L., Kay R. R 1988) **The search for morphogenes in Dictyostelium** *Bioessays* **9**:187–191

10. Bonner J. T 2008) **The social amoebae: the biology of cellular slime molds** USA: Princeton University Press

11. Bonner J. T., Suthers H. B., Odell G. M 1986) **Ammonia orients cell masses and speeds up aggregating cells of slime moulds** *Nature* **323**:630–632

12. Bonner J. T., Hoffman M. E 1963) **Evidence for a substance responsible for the spacing pattern of aggregation and fruiting in the cellular slime molds** *Development* **11**:571–589

13. Bose S., et al. 2020) **tRNA adenosine deaminase 3 is required for telomere maintenance in Arabidopsis thaliana** *Plant Cell Reports* **39**:1669–1685

14. Bradbury J. M., Gross J. D 1989) **The effect of ammonia on cell-type-specific enzyme accumulation in Dictyostelium discoideum** *Cell Differentiation and Development* **27**:121–128

15. Brady T. G., Hegarty V. J 1966) **An investigation of plant seeds for adenosine deaminase** *Nature* **209**:1027–1028

16. Brock D. A., Gomer R. H 1999) **A cell-counting factor regulating structure size in Dictyostelium** *Genes and Development* **13**:1960–1969

17. Brock D. A., Ehrenman K., Ammann R., Tang Y., Gomer R. H 2003) **Two components of a secreted cell number-counting factor bind to cells and have opposing effects on cAMP signal transduction in Dictyostelium** *Journal of Biological Chemistry* **278**:52262–52272

18. Burg A. W., Werner E 1975) **Effect of orally-administered caffeine and theophylline on tissue concentrations of 3', 5'cyclic-amp and phospho-diesterase** *Federation Proceedings* **34**:332–332

19. Carpousis A. J., Vanzo N. F., Raynal L. C 1999) **mRNA degradation: a tale of poly (A) and multiprotein machines** *Trends in Genetics* **15**:24–28

20. Carrin I., Murgia I., McLachlan A., Kay R. R 1996) **A mutational analysis of Dictyostelium discoideum multicellular development** *Microbiology* **142**:993–1003

21. Cha S., Agarwal R. P., Parks Jr R. E 1975) **Tight-binding inhibitors—II: Non-steady state nature of inhibition of milk xanthine oxidase by allopurinol and alloxanthine and of human erythrocytic adenosine deaminase by coformycin** *Biochemical Pharmacology* **24**:2187–2197

22. Chen Z. H., Schaap P 2012) **The prokaryote messenger c-di-GMP triggers stalk cell differentiation in Dictyostelium** *Nature* **488**:680–683

23. Chen Z. H., Schaap P 2016) **Secreted cyclic di-GMP induces stalk cell differentiation in the eukaryote Dictyostelium discoideum** *Journal of Bacteriology* **198**:27–31

24. Chen Z. H., Singh R., Cole C., Lawal H. M., Schilde C., Febrer M., Barton G. J., Schaap P 2017) **Adenylate cyclase A acting on PKA mediates induction of stalk formation by cyclic diguanylate at the Dictyostelium organizer** *Proceedings of the National Academy of Sciences USA* **114**:516–521

25. Chien S., Chung C. Y., Sukumaran S., Osborne N., Lee S., Ellsworth C., Mc Nally G. Y., Firtel R. A 2000) **The Dictyostelium LIM domain-containing protein LIM2 is essential for proper chemotaxis and morphogenesis** *Molecular Biology of the Cell* **11**:1275–1291

26. Cristalli G., Costanzi S., Lambertucci C., Lupidi G., Vittori S., Volpini R., Camaioni E 2001) **Adenosine deaminase: functional implications and different classes of inhibitors** *Medicinal Research Reviews* **21**:105–128

27. Coates J. C., Harwood A. J 2001) **Cell-cell adhesion and signal transduction during Dictyostelium development** *Journal of Cell Science* **114**:4349–4358

28. Conlay L. A., Evoniuk G., Wurtman R. J 1988) **Endogenous adenosine and hemorrhagic shock: effects of caffeine administration or caffeine withdrawal** *Proceedings of the National Academy of Sciences USA* **85**:4483–4485

29. Cotter D. A., Dunbar A. J., Buconjic S. D., Wheldrake J. F 1999) **Ammonium phosphate in sori of Dictyostelium discoideum promotes spore dormancy through stimulation of the osmosensor ACG** *Microbiology* **145**:1891–1901

30. Daly J. W, Garattini S 1993) **Mechanism of action of caffeine** *Caffeine, coffee, and health* Raven press :97–150

31. Davies L., Satre M., Martin J. B., Gross J. D 1993) **The target of ammonia action in Dictyostelium** *Cell* **75**:321–327

32. Dolezal T., Dolezelova E., Zurovec M., Bryant P. J 2005) **A role for adenosine deaminase in Drosophila larval development** *PLoS Biology* **3**:e201

33. Dunn J. D., Bosmani C., Barisch C., Raykov L., Lefrancois L. H., Cardenal-Munoz E., et al. 2018) **Eat prey, live: Dictyostelium discoideum as a model for cell-autonomous defenses** *Frontiers in Immunology* **8**:1906

34. Eichinger L, et al. 2005) **The genome of the social amoeba Dictyostelium discoideum** *Nature* **435**:43–57

35. Eidhammer I., Jonassen I., Taylor W. R 2000) **Structure comparison and structure patterns** *Journal of Computational Biology* **7**:685–716

36. Eng C. H., Yu K., Lucas J., White E., Abraham R. T 2010) **Ammonia derived from glutaminolysis is a diffusible regulator of autophagy** *Science signaling* **3**:119

37. Erdogan B., Ebbert P. T., Lowery L. A 2016) **Using Xenopus laevis retinal and spinal neurons to study mechanisms of axon guidance in vivo and in vitro** *Seminars in Cell and Developmental Biology* USA: Academic Press **51**:64–72

38. Farnsworth P 1973) **Morphogenesis in the cellular slime mould Dictyostelium discoideum; the formation and regulation of aggregate tips and the specification of developmental axes** *Development* **29**:253–266

39. Feit I. N 1988) **Ammonia can stimulate or inhibit aggregate density in Dictyostelium mucoroides: A quantitative test of the hypothesis that ammonia is the aggregation-suppressing gas** *Developmental Genetics*

40. Feit I. N., Medynski E. J., Rothrock M. J 2001) **Ammonia differentially suppresses the cAMP chemotaxis of anterior-like cells and prestalk cells in Dictyostelium discoideum** *Journal of Biosciences* **26**:157–166

41. Felsenstein J 1985) **Confidence limits on phylogenies: an approach using the bootstrap** *Evolution* **39**:783–791

42. Firtel R. A 1996) **Interacting signaling pathways controlling multicellular development in Dictyostelium** *Current Opinion in Genetics and Development* **6**:545–554

43. Follstaedt S. C., Kirsten J. H., Singleton C. K 2003) **Temporal and spatial expression of ammonium transporter genes during growth and development of Dictyostelium discoideum** *Differentiation* **71**:557–566

44. Gaspar H. B 2010) **Bone marrow transplantation and alternatives for adenosine deaminase deficiency** *Immunology and Allergy Clinics* **30**:221–236

45. Gee K., Russell F., Gross J. D 1994) **Ammonia hypersensitivity of slugger mutants of D. discoideum** *Journal of Cell Science* **107**:701–708

46. Gruenheit N., et al. 2021) **Mutant resources for functional genomics in Dictyostelium discoideum using REMI-seq technology** *BMC Biology* **19**:172

47. Hagmann J 1986) **Caffeine and heat shock induce adenylate cyclase in Dictyostelium discoideum** *The EMBO Journal* **5**:3437–3440

48. Hames B. D., Ashworth J. M 1974) **The metabolism of macromolecules during the differentiation of myxamoebae of the cellular slime mould Dictyostelium discoideum containing different amounts of glycogen** *Biochemical Journal* **142**:301–315

49. Hanif M. A., Hossen S., Cho Y., Sukhan Z. P., Choi C. Y., Kho K. H 2022) **Characterization and expression analysis of mollusk-like growth factor: A secreted protein involved in Pacific abalone embryonic and larval development** *Biology* **11**:1445

50. Harrison M. J 2005) **signaling in the arbuscular mycorrhizal symbiosis** *Annu. Rev. Microbiol* **59**:19–42

51. Helgason T., Daniell T. J., Husband R., Fitter A. H., Young J. P. W 1998) **Ploughing up the wood-wide web** *Nature* **394**:431–431

52. Hiraoka H., Wang J., Nakano T., Hirano Y., Yamazaki S., Hiraoka Y., Haraguchi T 2022) **ATP levels influence cell movement during the mound phase in Dictyostelium discoideum as revealed by ATP visualization and simulation** *FEBS Open bio* **12**:2042–2056

53. Honorato R. V., Koukos P. I., Jiménez-García B., Tsaregorodtsev A., Verlato M., Giachetti A., Rosato A., Bonvin A. M 2021) **Structural biology in the clouds: the WeNMR-EOSC ecosystem** *Frontiers in Molecular Biosciences* **8**:729513

54. Honorato R. V., Trellet M. E., Jiménez-García B., Schaarschmidt J. J., Giulini M., Reys V., Koukos P. I., Rodrigues J. P. G. L. M., Karaca E., van Zundert G. C. P., Roel-Touris J., van Noort C. W., Jandova Z., Melquiond A. S. J., Bonvin A. M. 2024) **The HADDOCK2. 4 web server for integrative modeling of biomolecular complexes.** *Nature Protocols* :1–23

55. Huber R. J., Williams R. S., Müller-Taubenberger A 2022) **Dictyostelium: A Tractable Cell and Developmental Model in Biomedical Research** *Frontiers in Cell and Developmental Biology* **10**:909619

56. Iijima R., Kunieda T., Yamaguchi S., Kamigaki H., Fujii-Taira I., Sekimizu K., Kubo T., Natori S., Homma K. J 2008) **The extracellular adenosine deaminase growth factor, ADGF/CECR1, plays a role in Xenopus embryogenesis via the adenosine/P1 receptor.** *J Biol Chem.* **283**:2255–2264

57. Inouye K 1989) **Control of cell type proportions by a secreted factor in Dictyostelium discoideum** *Development* **107**:605–609

58. Jumper J, et. al. 2021) **Highly accurate protein structure prediction with alphafold** *Nature* **596**:583–589

59. Kay R. R., Tilly R., Garrod D 1978) **Requirement for cell differentiation in Dictyostelium discoideum** *Nature* **271**:58–60

60. Kellerman K. A., McNally J. G 1999) **Mound-Cell Movement and Morphogenesis in Dictyostelium** *Developmental Biology* **208**:416–429

61. Kessin R. H 2001) **Dictyostelium: evolution, cell biology, and the development of multicellularity** Cambridge University Press

62. Khachatrian L., Klein C., Howlett A 1987) **Regulation of Dictyostelium discoideum adenylate cyclase by manganese and adenosine analogs** *Biochimica et Biophysica Acta (BBA)- Molecular Cell Research* **927**:235–246

63. Kirsten J. H., Xiong Y., Dunbar A. J., Rai M., Singleton C. K 2005) **Ammonium transporter C of Dictyostelium discoideum is required for correct prestalk gene expression and for regulating the choice between slug migration and culmination** *Developmental Biology* **287**:146–156

64. Koehl P 2001) **Protein structure similarities** *Current Opinion in Structural Biology* **11**:348–353

65. Konijn T. M., Van De Meene J. G., Bonner J. T., Barkley D. S. 1967) **The acrasin activity of adenosine-3', 5'-cyclic phosphate** *Proceedings of the National Academy of Sciences USA* **58**:1152–1154

66. Kosugi T., Inouye K 1989) **Negative chemotaxis to ammonia and other weak bases by migrating slugs of the cellular slime moulds** *Microbiology* **135**:1589–1598

67. Kumar S., Stecher G., Li M., Knyaz C., Tamura K 2018) **MEGA X: molecular evolutionary genetics analysis across computing platforms** *Molecular Biology and Evolution* **35**:1547

68. Lam T., Pickering G., Geltosky J., Siu C. H 1981) **Differential cell cohesiveness expressed by prespore and prestalk cells of Dictyostelium discoideum** *Differentiation* **20**:22–28

69. Lane M., Gardner D. K 2003) **Ammonium induces aberrant blastocyst differentiation, metabolism, pH regulation, gene expression and subsequently alters fetal development in the mouse** *Biology of Reproduction* **69**:1109–1117

70. Letunic I., Bork P 2018) **20 years of the SMART protein domain annotation resource** *Nucleic Acids Research* **46**:D493–D496

71. Lipkowski J., Galus Z 1973) **Electrode kinetics in mixed solvents Investigations of the kinetics and equilibrium properties of manganese (II)—ammonia complexes in water and mixed solvents of n-propanol, isopropanol, t-butanol and water** *Journal of Electroanalytical Chemistry and Interfacial Electrochemistry* **48**:337–352

72. Liu Y., Zhang X., Wang W., Liu T., Ren J., Chen S., Lu T., Yuan X., Mo F., Yang J, Wei Y., Wei X 2022) **Ammonia promotes the proliferation of bone marrow-derived mesenchymal stem cells by regulating the Akt/mTOR/S6k pathway** *Bone Research* **10**:57

73. Lonski J 1976) **The effect of ammonia on fruiting body size and microcyst formation in the cellular slime molds** *Developmental Biology* **51**:158–165

74. Loomis W. F., Klein C., Bracket P 1979) **The effect of divalent cations on aggregation of Dictyostelium discoideum** *Differentiation* **12**:83–89

75. Lu J., Li Y., Zhang C., Yang X., Qiang J. W 2020) **Interaction of manganese and ammonia in the brain of hepatic encephalopathy rats** *Hepatitis Monthly* **20**:8

76. Mahadeo D. C., Parent C. A 2006) **Signal relay during the life cycle of Dictyostelium** *Current topics in Developmental Biology* **73**:115–140

77. Maier S. A., Galellis J. R., McDermid H. E 2005) **Phylogenetic analysis reveals a novel protein family closely related to adenosine deaminase** *Journal of Molecular Evolution* **61**:776–794

78. Mann S. K., Firtel R. A 1993) **cAMP-dependent protein kinase differentially regulates prestalk and prespore differentiation during Dictyostelium development** *Development* **119**:135–146

79. Marone G., Plaut M., Lichtenstein L. M 1980) **The role of adenosine in the control of immune function** *Ricerca in clinica e in laboratorio* **10**:303–312

80. Martín-González J., Montero-Bullón J. F., Lacal J. 2021) **Dictyostelium discoideum as a non-mammalian biomedical model** *Microbial Biotechnology* **14**:111–125

81. Mizushima N., Levine B., Cuervo A. M., Klionsky D. J 2008) **Autophagy fights disease through cellular self-digestion** *Nature* **451**:1069–1075

82. Moreno E., Canet J., Gracia E., Lluís C., Mallol J., Canela E. I., Cortés A., Casadó V. 2018) **Molecular Evidence of Adenosine Deaminase Linking Adenosine A2A Receptor and CD26 Proteins** *Frontiers in Pharmacology* **9**:106

83. Müller-Taubenberger A., Kortholt A., Eichinger L 2013) **Simple system–substantial share: the use of Dictyostelium in cell biology and molecular medicine** *European Journal of Cell Biology* **92**:45–53

84. Nassir N., Hyde G. J., Baskar R 2019) **A telomerase with novel non-canonical roles: TERT controls cellular aggregation and tissue size in Dictyostelium** *PLoS Genetics* **15**:e1008188

85. Feit I. N, Bonner J. T., Suthers H. B. 1990) **Regulation of the anterior-like cell state by ammonia in Dictyostelium discoideum** *Developmental Genetics*

86. Neave N., Sobolewski A., Weeks G 1983) **The effect of ammonia on stalk cell formation in submerged monolayers of Dictyostelium discoideum** *Cell Differentiation* **13**:301–307

87. Needham J 1926) **The energy-sources in ontogenesis: III. The ammonia content of the developing avian egg and the theory of recapitulation** *Journal of Experimental Biology* **4**:145–154

88. Newell P. C., Telser A., Sussman M 1969) **Alternative developmental pathways determined by environmental conditions in the cellular slime mold Dictyostelium discoideum** *Journal of Bacteriology* **100**:763–768

89. Newell P. C 1982) **Cell surface binding of adenosine to Dictyostelium and inhibition of pulsatile signaling** *FEMS Microbiology Letters* **13**:417–421

90. Notarangelo L. D 2016) **T cell immunodeficiencies. Paediatric Allergy** *E-Book: Principles and Practice*

91. Otto G. P., Wu M. Y., Kazgan N., Anderson O. R., Kessin R. H 2003) **Macroautophagy is required for multicellular development of the social amoeba Dictyostelium discoideum** *Journal of Biological Chemistry* **278**:17636–17645

92. Otto G. P., Wu M. Y., Clarke M., Lu H., Anderson O. R., Hilbi H., Shuman H, and Kessin A, H R. 2004) **Macroautophagy is dispensable for intracellular replication of Legionella pneumophila in Dictyostelium discoideum** *Molecular Microbiology* **51**:63–72

93. Palsson E., Cox E. C 1996) **Origin and evolution of circular waves and spirals in Dictyostelium discoideum territories** *Proceedings of the National Academy of Sciences USA*

93:1151–1155

94. Pijuan-Sala B., Griffiths J. A., Guibentif C., Hiscock T. W., Jawaid W., Calero-Nieto F. J., Mulas C., Ibarra-Soria X., Tyser R. C. V, Ho D. L. L., Reik W., Srinivas S., Simons D. B., Nichols J., Marioni J.C., Göttgens B 2019) **A single-cell molecular map of mouse gastrulation and early organogenesis** *Nature* **566**:490–495

95. Raper K. B 1940) **Pseudoplasmodium formation and organization in Dictyostelium discoideum** *Journal of the Elisha Mitchell Scientific Society* **56**:241–282

96. Riazi A. M., Arsdell G. V., Buchwald M 2005) **Transgenic expression of CECR1 adenosine deaminase in mice results in abnormal development of heart and kidney** *Transgenic Research* **14**:333–336

97. Riley B. B., Barclay S. L 1990) **Ammonia promotes accumulation of intracellular cAMP in differentiating amoebae of Dictyostelium discoideum** *Development* **109**:715–722

98. Rivera-Mancía S., Ríos C., Montes S 2012) **Manganese and ammonia interactions in the brain of cirrhotic rats: effects on brain ammonia metabolism** *Neurochemical Research* **37**:1074–1084

99. Roisin-Bouffay C., Jang W., Caprette D. R., Gomer R. H 2000) **A precise group size in Dictyostelium is generated by a cell-counting factor modulating cell–cell adhesion** *Molecular Cell* **6**:953–959

100. Rubin J., Robertson A 1975) **The tip of the Dictyostelium discoideum pseudoplasmodium as an organizer** *Development* **33**:227–241

101. Saitou N., Nei M 1987) **The neighbor-joining method: a new method for reconstructing phylogenetic trees** *Molecular Biology and Evolution* **4**:406–425

102. Saxe C.., Ginsburg G. T., Louis J. M., Johnson R., Devreotes P. N., Kimmel A. R. 1993) **CAR2, a prestalk cAMP receptor required for normal tip formation and late development of Dictyostelium discoideum.** *Genes and Development* **7**:262–272

103. Schaap P., Brandt R., van Es S. 1995) **Regulation of Dictyostelium adenylylcyclases by morphogen-induced modulation of cytosolic pH or Ca2+ levels** *Developmental Biology* **168**:179–188

104. Schaap P., Wang M 1986) **Interactions between adenosine and oscillatory cAMP signaling regulate size and pattern in Dictyostelium** *Cell* **45**:137–144

105. Schindler J., Sussman M 1977) **Ammonia determines the choice of morphogenetic pathways in Dictyostelium discoideum** *Journal of Molecular Biology* **116**:161–169

106. Schindler J., Sussman M 1979) **Inhibition by ammonia of intracellular cAMP accumulation in Dictyostelium discoideum: its significance for the regulation of morphogenesis** *Developmental Genetics* **1**:13–20

107. Schmittgen T. D., Livak K. J 2008) **Analyzing real-time PCR data by the comparative CT method** *Nature protocols* **3**:1101–1108

108. Schulz-Bohm K., Martín-Sánchez L., Garbeva P 2017) **Microbial volatiles: small molecules with an important role in intra and inter-kingdom interactions** *Frontiers in Microbiology*

8:289291

109. Schultz R. D., Gumienny T. L 2012) **Visualization of Caenorhabditis elegans cuticular structures using the lipophilic vital dye DiI** *Journal of Visualized Experiments* **59**:e3362

110. Siegert F., Weijer C 1989) **Digital image processing of optical density wave propagation in Dictyostelium discoideum and analysis of the effects of caffeine and ammonia** *Journal of Cell Science* **93**:325–335

111. Siegert F., Weijer C. J 1995) **Spiral and concentric waves organize multicellular Dictyostelium mounds** *Current Biology* **5**:937–943

112. Singer G., Araki T., Weijer C. J 2019) **Oscillatory cAMP cell-cell signaling persists during multicellular Dictyostelium development** *Communications Biology* **2**:139

113. Singh S. P., Insall R. H, Chang C, Wang J 2022) **Under-Agarose Chemotaxis Chemotaxis and Migration Assays for Dictyostelium** *Cell Polarity Signaling: Methods and Protocols* New York, NY: Springer US :467–482

114. Singleton C. K., Zinda M. J., Mykytka B., Yang P 1998) **The histidine kinase dhkC regulates the choice between migrating slugs and terminal differentiation in Dictyostelium discoideum** *Developmental Biology* **203**:345–357

115. Singleton C. K., Kirsten J. H., Dinsmore C. J 2006) **Function of ammonium transporter A in the initiation of culmination of development in Dictyostelium discoideum** *Eukaryotic Cell* **5**:991–996

116. Singleton C. K., Xiong Y 2013) **Loss of the histidine kinase DhkD results in mobile mounds during development of Dictyostelium discoideum** *Plos One* **8**:e75618

117. Siu C. H., Lam T. Y., Choi A. H 1985) **Inhibition of cell-cell binding at the aggregation stage of Dictyostelium discoideum development by monoclonal antibodies directed against an 80,000-dalton surface glycoprotein** *Journal of Biological Chemistry* **260**:16030–16036

118. Steer M. L 1975) **Adenyl cyclase** *Annals of Surgery* **182**:603

119. Stege J. T., Laub M. T., Loomis W. F 1999) **Tip genes act in parallel pathways of early Dictyostelium development** *Developmental Genetics* **25**:64–77

120. Stein L. Y., Campbell M. A., Klotz M. G 2013) **Energy-mediated vs. ammonium- regulated gene expression in the obligate ammonia-oxidizing bacterium, Nitrosococcus oceani** *Frontiers in Microbiology* **4**:277

121. Sternfeld J., David C. N 1982) **Fate and regulation of anterior-like cells in Dictyostelium slugs** *Developmental Biology* **93**:111–118

122. Storey C. L., Williams R. S. B., Fisher P. R., Annesley S. J 2022) **Dictyostelium discoideum: A model system for neurological disorders** *Cells* **11**:463

123. Tanaka T., Kameoka J., Yaron A., Schlossman S. F., Morimoto C 1993) **The costimulatory activity of the CD26 antigen requires dipeptidyl peptidase IV enzymatic activity** *Proceedings of the National Academy of Sciences USA* **90**:4586–4590

124. Taya Y., Tanaka Y., Nishimura S 1978) **5'-AMP is a direct precursor of cytokinin in Dictyostelium discoideum** *Nature* **271**:545–547

125. Thadani V., Pan P., Bonner J. T 1977) **Complementary effects of ammonia and cAMP on aggregation territory size in the cellular slime mold Dictyostelium mucoroides** *Experimental Cell Research* **108**:75–78

126. Theibert A., Devreotes P. N 1984) **Adenosine and its derivatives inhibit the cAMP signaling response in Dictyostelium discoideum** *Developmental Biology* **106**:166–173

127. Thomason P., Traynor D., Kay R 1999) **Taking the plunge: terminal differentiation in Dictyostelium** *Trends in Genetics* **15**:15–19

128. Thompson C. R., Kay R. R 2000) **The role of DIF-1 signaling in Dictyostelium development** *Molecular Cell* **6**:1509–1514

129. Traynor D., Kessin R. H., Williams J. G 1992) **Chemotactic sorting to cAMP in the multicellular stages of Dictyostelium development** *Proceedings of the National Academy of Sciences USA* **89**:8303–8307

130. Tung S. M., Ünal C., Ley A., Peña C., Tunggal B., Noegel A. A., Krut O., Steinert M., Eichinger L 2010) **Loss of Dictyostelium ATG9 results in a pleiotropic phenotype affecting growth, development, phagocytosis and clearance and replication of Legionella pneumophila** *Cellular Microbiology* **12**:765–780

131. Tyser R. C., Mahammadov E., Nakanoh S., Vallier L., Scialdone A., Srinivas S 2021) **Single-cell transcriptomic characterization of a gastrulating human embryo** *Nature* **600**:285–289

132. Tzertzinis G., Ganatra M. B., Ruse C., Taron C. H., Causey B., Wang L., Schildkraut I 2023) **The AMP deaminase of the mollusk Helix pomatia is an unexpected member of the adenosine deaminase-related growth factor (ADGF) family** *PloS One* **18**:e0286435

133. Van Haastert P. J. 1983) **Binding of cAMP and adenosine derivatives to Dictyostelium discoideum cells. Relationships of binding, chemotactic, and antagonistic activities** *Journal of Biological Chemistry* **258**:9643–9648

134. Wakamiya M., Blackburn M. R., Jurecic R., McArthur M. J., Geske R. S., Cartwright Jr J., Kellems R. E 1995) **Disruption of the adenosine deaminase gene causes hepatocellular impairment and perinatal lethality in mice** *Proceedings of the National Academy of Sciences USA* **92**:3673–3677

135. Walsh J., Wright B. E 1978) **Kinetics of net RNA degradation during development in Dictyostelium discoideum** *Microbiology* **108**:57–62

136. Wang B., Kuspa A 2002) **CulB, a putative ubiquitin ligase subunit, regulates prestalk cell differentiation and morphogenesis in Dictyostelium spp** *Eukaryotic Cell* **1**:126–136

137. Wang M., Schaap P 1985) **Correlations between tip dominance, prestalk/prespore pattern, and cAMP-relay efficiency in slugs of Dictyostelium discoideum** *Differentiation* **30**:7–14

138. Wang M., Schaap P 1989) **Ammonia depletion and DIF trigger stalk cell differentiation in intact Dictyostelium discoideum slugs** *Development* **105**:569–574

139. Weijer C. J 2009) **Collective cell migration in development** *Journal of Cell Science* **122**:3215–3223

140. White G. J., Sussman M 1961) **Metabolism of major cell components during slime mold morphogenesis** *Biochimica et biophysica acta* **53**:285–293

141. Wiechetek M., Breves G., Höller H 1979) **The effect of ammonium ion concentration on the activity of adenylate cyclase in various rat tissues in vitro** *Quarterly Journal of Experimental Physiology and Cognate Medical Sciences: Translation and Integration* **64**:169–174

142. Williams G. B., Elder E. M., Sussman M 1984) **Modulation of the cAMP relay in Dictyostelium discoideum by ammonia and other metabolites: possible morphogenetic consequences** *Developmental Biology* **105**:377–388

143. Williams J. G 1988) **The role of diffusible molecules in regulating the cellular differentiation of Dictyostelium discoideum** *Development* **103**:1–16

144. Williams J. G 2006) **Transcriptional regulation of Dictyostelium pattern formation** *EMBO Reports* **7**:694–698

145. Williams J. G., Duffy K. T., Lane D. P., McRobbie S. J., Harwood A. J., Traynor D., Kay R. R., Jermyn K. A 1989) **Origins of the prestalk-prespore pattern in Dictyostelium development** *Cell* **59**:1157–1163

146. Xu J., Wang X., Chen J., Chen S., Li Z., Liu H., Bai Y, Zhi F 2020) **Embryonic stem cell-derived mesenchymal stem cells promote colon epithelial integrity and regeneration by elevating circulating IGF-1 in colitis mice** *Theranostics* **10**:12204

147. Yamada T 1950) **Dorsalization of the ventral marginal zone of the Triturus gastrula. I. Ammonia-treatment of the medio-ventral marginal zone** *The Biological bulletin* **98**:98–121

148. Yeung S. M. H., Shoshani I., Stübner D., Johnson R. A 1989) **Ammonium ions enhance proteolytic activation of adenylate cyclase and decrease its sensitivity to inhibition by "P"-site agonists** *Archives of Biochemistry and Biophysics* **271**:332–345

149. Yoshino R., Morio T., Yamada Y., Kuwayama H., Sameshima M., Tanaka Y., Sesaki H., Iijima M 2007) **Regulation of ammonia homeostasis by the ammonium transporter AmtA in Dictyostelium discoideum** *Eukaryotic Cell* **6**:2419–2428

150. Zavialov A. V., Yu X., Spillmann D., Lauvau G., Zavialov A. V 2010) **Structural basis for the growth factor activity of human adenosine deaminase ADA2** *Journal of Biological Chemistry* **285**:12367–12377

151. Zhou Q, et al. 2014) **Early-onset stroke and vasculopathy associated with mutations in ADA2** *New England Journal of Medicine* **370**:911–920

152. Zurovec M., Dolezal T., Gazi M., Pavlova E., Bryant P. J 2002) **Adenosine deaminase- related growth factors stimulate cell proliferation in Drosophila by depleting extracellular adenosine** *Proceedings of the National Academy of Sciences USA* **99**:4403–4408

Author information

Pavani Hathi
Bhupat and Jyoti Mehta School of Biosciences, Department of Biotechnology, Indian Institute of Technology-Madras, Chennai, India

Ramamurthy Baskar
Bhupat and Jyoti Mehta School of Biosciences, Department of Biotechnology, Indian Institute of Technology-Madras, Chennai, India
ORCID iD: 0000-0001-5705-9976

For correspondence: rbaskar@iitm.ac.in

Editors

Reviewing Editor
K VijayRaghavan
National Centre for Biological Sciences, Tata Institute of Fundamental Research, Bangalore, India

Senior Editor
K VijayRaghavan
National Centre for Biological Sciences, Tata Institute of Fundamental Research, Bangalore, India

Reviewer #1 (Public review):

Summary:

This work shows that a specific adenosine deaminase protein in Dictyostelium generates the ammonia that is required for tip formation during Dictyostelium development. Cells with an insertion in the ADGF gene aggregate but do not form tips. A remarkable result, shown in several different ways, is that the ADGF mutant can be rescued by exposing the mutant to ammonia gas. The authors also describe other phenotypes of the ADGF mutant such as increased mound size, altered cAMP signaling, and abnormal cell type differentiation. It appears that the ADGF mutant has defects in the expression of a large number of genes, resulting in not only the tip defect but also the mound size, cAMP signaling, and differentiation phenotypes.

Strengths:

The data and statistics are excellent.

Weaknesses:

The key weakness is understanding why the cells bother to use a diffusible gas like ammonia as a signal to form a tip and continue development. The rescue of the mutant by adding ammonia gas to the entire culture indicates that ammonia conveys no positional information within the mound. By the time the cells have formed a mound, the cells have been starving for several hours, and desperately need to form a fruiting body to disperse some of themselves as spores, and thus need to form a tip no matter what. One can envision that the local ammonia concentration is possibly informing the mound that some minimal number of cells are present (assuming that the ammonia concentration is proportional to the number of

cells), but probably even a minuscule fruiting body would be preferable to the cells compared to a mound. This latter idea could be easily explored by examining the fate of the ADGF cells in the mound - do they all form spores? Do some form spores? Or perhaps the ADGF is secreted by only one cell type, and the resulting ammonia tells the mound that for some reason that cell type is not present in the mound, allowing some of the cells to transdifferentiate into the needed cell type. Thus elucidating if all or some cells produce ADGF would greatly strengthen this puzzling story.

https://doi.org/10.7554/eLife.104855.1.sa2

Reviewer #2 (Public review):

Summary:

The paper describes new insights into the role of adenosine deaminase-related growth factor (ADGF), an enzyme that catalyses the breakdown of adenosine into ammonia and inosine, in tip formation during Dictyostelium development. The ADGF null mutant has a pre-tip mound arrest phenotype, which can be rescued by the external addition of ammonia. Analysis suggests that the phenotype involves changes in cAMP signaling possibly involving a histidine kinase dhkD, but details remain to be resolved.

Strengths:

The generation of an ADGF mutant showed a strong mound arrest phenotype and successful rescue by external ammonia. Characterisation of significant changes in cAMP signaling components, suggesting low cAMP signaling in the mutant and identification of the histidine kinase dhkD as a possible component of the transduction pathway. Identification of a change in celltype differentiation towards prestalk fate

Weaknesses:

Lack of details on the developmental time course of ADGF activity and celltype type-specific differences in ADGF expression. The absence of measurements to show that ammonia addition to the null mutant can rescue the proposed defects in cAMP signaling. No direct measurements in the dhkD mutant to show that it acts upstream of sdgf in the control of changes in cAMP signaling and tip formation.

https://doi.org/10.7554/eLife.104855.1.sa1

Author response:

> ***Public Reviews:***
>
> ***Reviewer #1 (Public review):***
>
> *Summary:*
>
> *This work shows that a specific adenosine deaminase protein in* Dictyostelium *generates the ammonia that is required for tip formation during* Dictyostelium *development. Cells with an insertion in the ADGF gene aggregate but do not form tips. A remarkable result, shown in several different ways, is that the ADGF mutant can be rescued by exposing the mutant to ammonia gas. The authors also describe other phenotypes of the ADGF mutant such as increased mound size, altered cAMP signalling, and abnormal cell type differentiation. It appears that the ADGF mutant has defects in the expression of a large*

> *number of genes, resulting in not only the tip defect but also the mound size, cAMP signalling, and differentiation phenotypes.*
>
> *Strengths:*
>
> *The data and statistics are excellent.*
>
> *Weaknesses:*
>
> *(1) The key weakness is understanding why the cells bother to use a diffusible gas like ammonia as a signal to form a tip and continue development.*

Ammonia serves as a crucial signalling molecule influencing both multicellular organization and differentiation in *Dictyostelium* (Francis, 1964; Bonner et al., 1989; Bradbury and Gross, 1989). Ammonia by raising the pH of the intracellular acidic vesicles of prestalk cells (Poole and Ohkuma, 1981; Gross et al, 1983), and the cytoplasm, is known to increase the speed of chemotaxing amoebae (Siegert and Weijer 1989; Van Duijn and Inouye, 1991), triggering multicellular movement (Bonner et al., 1988, 1989), favoring tipped mound development. The slug tip is known to release ammonia and the slime sheath at the back of the slug prevents diffusion (Bonner et al., 1989) and thus high ammonia levels at the back, help prespore differentiation (Newell et al., 1969). Ammonia favors slug migration than fruiting (Schindler and Sussman, 1977) and thus, ammonia coming from the tip may favor synchronized development of the entire colony. The tip exerts negative chemotaxis towards ammonia probably helping the slugs to move away from each other ensuring equal spacing of the fruiting bodies (Feit and Sollitto, 1987).

Ammonia released in pulses acts as a long-distance signalling molecule between colonies of yeast cells indicating depletion of nutrient resources and promoting synchronous development (Palkova et al., 1997; Palkova and Forstova, 2000). Similarly, ammonia diffusion may influence neighboring *Dictyostelium* colonies. Ammonia produced in millimolar concentrations (Schindler and Sussman, 1977) could ward off other predators in soil. For instance, ammonia released by *Streptomyces* symbionts of leaf-cutting ants is known to inhibit fungal pathogens (Dhodary and Spiteller, 2021). Additionally, ammonia recycling into amino acids, as observed in breast cancer proliferation (Spinelli et al., 2017), may also occur in starving *Dictyostelium* cells, supporting survival and differentiation. These findings suggest that ammonia acts as both a local and long-range regulatory signal, integrating environmental and cellular cues to coordinate multicellular development.

> *(2) The rescue of the mutant by adding ammonia gas to the entire culture indicates that ammonia conveys no positional information within the mound.*

Ammonia is known to influence rapid patterning of *Dictyostelium* cells confined in a restricted environment (Sawai et al., 2002). Both neutral red staining (a marker for prestalk and ALCs) (Fig. S2) and the prestalk marker *ecmA/ ecmB* expression (Fig. 8C) in the *adgf* mutants suggest that the mounds have differentiated prestalk cells but are blocked in development. The mound arrest phenotype can be reversed by exposing the *adgf* mutant mounds to ammonia.

Based on cell cycle phases, there exists a dichotomy of cell types, that biases cell fate as prestalk or prespore (Weeks and Weijer, 1994; Jang and Gomer, 2011). Prestalk cells are enriched in acidic vesicles, and ammonia, by raising the pH of these vesicles and the cytoplasm (Davies et al 1993; Van Duijn and Inouye 1991), plays an active role in collective cell movement (Bonner et al., 1989). Thus, ammonia reinforces or maintains the positional information by elevating cAMP levels, favoring prespore differentiation (Bradbury and Gross, 1989; Riley and Barclay, 1990; Hopper et al., 1993).

> *(3) By the time the cells have formed a mound, the cells have been starving for several hours, and desperately need to form a fruiting body to disperse some of themselves as spores, and thus need to form a tip no matter what.*

When the *adgf* mutants were exposed to ammonia just after tight mound formation, tips developed within 4 h (Fig. 6). In contrast, *adgf* mounds, not exposed to ammonia remained at the mound stage for at least 30 h. This demonstrates that starvation alone is not sufficient to drive tip development and ammonia serves as a cue that promotes the transition from mound to tipped mound formation.

Many mound arrest mutants are blocked in development and do not proceed to form fruiting bodies (Carrin et al., 1994). Further, not all the mound arrest mutants tested in this study were rescued by ADA enzyme (Fig. S3 A), and they continue to stay as mounds without dispersing as spores.

> *(4) One can envision that the local ammonia concentration is possibly informing the mound that some minimal number of cells are present (assuming that the ammonia concentration is proportional to the number of cells), but probably even a minuscule fruiting body would be preferable to the cells compared to a mound. This latter idea could be easily explored by examining the fate of the ADGF cells in the mound - do they all form spores? Do some form spores?*
>
> *Or perhaps the ADGF is secreted by only one cell type, and the resulting ammonia tells the mound that for some reason that cell type is not present in the mound, allowing some of the cells to transdifferentiate into the needed cell type. Thus, elucidating if all or some cells produce ADGF would greatly strengthen this puzzling story.*

A fraction of *adgf* mounds form bulkier spore heads by the end of 36 h as shown in Fig. 3. This late recovery may be due to the expression of other ADA isoforms. Mixing WT and *adgf* mutant cell lines results in a slug with the mutants occupying the prestalk region (Fig. 9) suggesting that WT ADGF favours prespore differentiation. However, it is not clear if ADGF is secreted by a particular cell type, as adenosine can be produced by both cell types, and the activity of three other intracellular ADAs may vary between the cell types. To address whether *adgf* expression is cell type-specific, prestalk and prespore cells will be isolated, and thereafter, *adgf* expression in each population will be examined.

ADGF activity is likely to be higher in the tip to remove excess adenosine, the tip-inhibiting molecule (Wang and Schaap, 1985), and our results also show that *adgf* - cells with high adenosine preferentially migrate to the prestalk than the prespore region when mixed with WT cells. Ammonia generated from adenosine deamination could thus drive tip development and prespore differentiation.

> ***Reviewer #2 (Public review):***
>
> *Summary:*
>
> *The paper describes new insights into the role of adenosine deaminase-related growth factor (ADGF), an enzyme that catalyses the breakdown of adenosine into ammonia and inosine, in tip formation during Dictyostelium development. The ADGF null mutant has a pre-tip mound arrest phenotype, which can be rescued by the external addition of ammonia. Analysis suggests that the phenotype involves changes in cAMP signalling possibly involving a histidine kinase dhkD, but details remain to be resolved.*
>
> *Strengths:*

> *The generation of an ADGF mutant showed a strong mound arrest phenotype and successful rescue by external ammonia. Characterization of significant changes in cAMP signalling components, suggesting low cAMP signalling in the mutant and identification of the histidine kinase dhkD as a possible component of the transduction pathway. Identification of a change in cell type differentiation towards prestalk fate*
>
> *Weaknesses:*
>
> *(1) Lack of details on the developmental time course of ADGF activity and cell type type-specific differences in ADGF expression.*

ADGF expression was examined at 0, 8, 12, and 16 h (Fig. 1), and the total ADA activity was assayed at 12 and 16 h (Fig. 4). Previously, the 12 h data was not included, but it has now been added (Fig. 4A). The *adgf* expression was found to be highest at 16 h and hence, the ADA assay was carried out at that time point. Since the ADA assay will also report the activity of other three isoforms, it will not exclusively reflect ADGF activity.

A fraction of *adgf* - mounds form bulkier spore heads by the end of 36 h as shown in Fig. 3. This late recovery may be due to the expression of the other ADA isoforms. Mixing WT and *adgf* mutant cell lines results in a slug with the mutants occupying the prestalk region (Fig. 9) suggesting that WT *adgf* favours prespore differentiation. However, it's not clear if ADGF is secreted by a particular cell type, as adenosine can be produced by both cell types, and the activity of the other three intracellular ADAs may vary between the cell types. To address whether *adgf* expression is cell type-specific, prestalk and prespore cells will be isolated, and thereafter, *adgf* expression in each population will be examined.

ADGF activity is likely to be higher in the tip to remove excess adenosine, the tip-inhibiting molecule (Wang and Schaap, 1985), and our results also show that *adgf* - cells with high adenosine preferentially migrate to the prestalk than the prespore region when mixed with WT cells.

> *(2) The absence of measurements to show that ammonia addition to the null mutant can rescue the proposed defects in cAMP signalling.*

The cAMP levels were measured at two time points 8 h and 12 h in the mutant. The *adgf* mutant in comparison to WT has lower ammonia levels (Fig. 6), diminished *acaA* expression (Fig. 7) and reduced cAMP levels (Fig. 7) both at 12 and 16 h of development. Ammonia is known to increase cAMP levels (Riley and Barclay, 1990; Feit et al., 2001). Thus, ammonia addition to the mutant is likely to increase *acaA* expression, thus increase cAMP levels (Riley and Barclay, 1990; Feit et al., 2001) thereby rescuing the defects in cAMP signalling.

> *(3) No direct measurements in the dhkD mutant to show that it acts upstream of adgf in the control of changes in cAMP signalling and tip formation.*

The histidine kinases *dhkD* and *dhkC* are reported to modulate phosphodiesterase RegA activity, thereby maintaining cAMP levels (Singleton et al., 1998; Singleton and Xiong, 2013). By activating RegA, *dhkD* ensures proper cAMP distribution within the mound, which is essential for the patterning of prestalk and prespore cells, as well as for tip formation (Singleton and Xiong, 2013). Therefore, ammonia exposure to *dhkD* mutants is likely to regulate cAMP signalling and thereby tip formation.

https://doi.org/10.7554/eLife.104855.1.sa0